0013-7227/05/$15.00/0
Printed in U.S.A.

Endocrinology 146(3):1268–1284

doi: 10.1210/en.2004-1194

AQ: A

Regulation of Sertoli-Germ Cell Adherens Junction Dynamics via Changes in Protein-Protein Interactions of the *N*-Cadherin-β-Catenin Protein Complex which Are Possibly Mediated by c-Src and Myotubularin-Related Protein 2: An *in Vivo* Study Using an Androgen Suppression Model

Jiayi Zhang, Ching-hang Wong, Weiliang Xia, Dolores D. Mruk, Nikki P. Y. Lee, Will M. Lee, and C. Yan Cheng

Population Council (J.Z., C.W., W.X., D.D.M., N.P.Y.L., C.Y.C.), Center for Biomedical Research, New York, New York 10021; and Department of Zoology (W.M.L.), The University of Hong Kong, Hong Kong, China

Using a well characterized model of cell-cell actin-based adherens junction (AJ) disruption by suppressing the intratesticular testosterone level in adult rats with testosterone-
AQ: B **estradiol implants, we have confirmed earlier findings that Sertoli-germ cell AJ dynamics are regulated by the activation of kinases via putative signaling pathways but with some unexpected findings as follows. First, the loss of germ cells from the seminiferous epithelium during androgen suppression was associated with a surge in myotubularin-related protein 2 (MTMR2, a lipid phosphatase, in which adult MTMR2$^{-/-}$ mice were recently shown to be azoospermic because of the loss of cell adhesion function between germ and Sertoli cells); kinases: phosphatidylinositol 3-kinase, c-Src, and C-terminal**
AQ: C **Src kinase; adaptors: α-actinin, vinculin, afadin, and p130 Crk-associated protein; and AJ-integral membrane proteins at the ectoplasmic specialization (ES, a testis-specific cell-cell actin-based AJ type) site: *N*-cadherin, β-catenin, integrin β1, and nectin 3. Second, MTMR2, instead of structurally interacting with phosphatidylinositol 3-kinase, a protein and lipid kinase, was shown to associate only with c-Src, a nonreceptor protein tyrosine kinase, as demonstrated by both coimmunoprecipitation and fluorescent microscopy at the site of apical ES, but none of the kinases, adaptors, and AJ-integral proteins that were examined. Collectively, these results suggest that the MTMR2/c-Src is an important phosphatase/kinase protein pair in AJ dynamics in the testis. Because c-Src is known to associate with the cadherin/catenin protein complex at the ES in the testis, we next sought to investigate any changes in the protein-protein interactions of this protein complex during androgen suppression-induced germ cell loss. Indeed, there was a loss of *N*-cadherin and β-catenin association, accompanied by a surge in Tyr phosphorylation of β-catenin, during germ cell loss from the epithelium. Third, and perhaps the most important of all, during natural recovery of the epithelium after removal of testosterone-estradiol implants when spermatids were reattaching to Sertoli cells, an increase in *N*-cadherin and β-catenin association was detected with a concomitant loss in the increased Tyr phosphorylation in β-catenin. In summary, these results illustrate that the cadherin/catenin is a crucial cell adhesion complex that regulates AJ dynamics in the testis, and its functionality is likely modulated by the MTMR2/c-Src protein complex. (*Endocrinology* 146: 1268–1284, 2005)**

IN THE MAMMALIAN TESTIS, SUCH as in the rat, spermatogenesis takes place in the seminiferous epithelium in which one type A1 spermatogonium (diploid, 2n) divides and differentiates into 256 spermatids (haploid, 1n). This event is associated with extensive junction restructuring so as to facilitate germ cell movement, because germ cells must traverse the epithelium, translocating from the basal to the adluminal compartment. As such, fully developed spermatids can be released to the tubule lumen at spermiation (for reviews, see Refs. 1–3). If this event can be disrupted, spermatogenesis will be compromised, leading to male infertility. Indeed, new approaches to disrupt tight junction and adherens junction (AJ) dynamics are being widely investigated for identifying novel male contraceptives (for reviews, see Refs. 2, 3). 1-(2,4-Dichlorobenzyl)-indazole-3-carbohydrazide (AF-2364, also known as Adjudin, a molecule that induces Sertoli-germ cell AJ disruption) (3, 4) is one of these novel compounds that was synthesized based on the core structure of indazole-3-carboxylic acid known to possess potent antispermatagenic effects (for a review, see Ref. 5). Furthermore, the toxic effects of AF-2364 were low when it was administered once weekly (6–8). Recent studies have shown that AF-2364-induced AJ disruption is a potential reversible male contra-

First Published Online December 9, 2004

Abbreviations: AJ, Adherens junction; BW, body weight; CK, casein kinase; CMT, Charcot-Marie-Tooth disease; CPA, cyproterone acetate; Csk, C-terminal Src kinase; DAPI, 4′,6-diamidino-2-phenylindole; Dlg1, disc large 1; E, estradiol-17β; ES, ectoplasmic specialization; FITC, fluorescein isothiocyanate; IP, immunoprecipitation; MTM, myotubularin; MTMR2, myotubularin-related protein 2; NR, spontaneous natural recovery; PI 3-K, phosphatidylinositol 3-kinase; PTP, protein tyrosine phosphatase, r, rat; T, testosterone; *T*, total gel concentration (g/100 ml) = acrylamide + methylene bisacrylamide; TE, testosterone-estradiol; ZO-1, zonula occludens 1.

Endocrinology **is published monthly by The Endocrine Society (http://www.endo-society.org), the foremost professional society serving the endocrine community.**

balt3/zee-end/zee-end/zee00305/zee0730-05a | hurtr | S=12 | 1/21/05 | 7:52 | 4/Color Figure(s): 1,2,3,6,10 | Art: 1195093 | Input-lc

ceptive, which can also be used as an *in vivo* model to study AJ dynamics in the testis (for reviews, see Refs. 2, 3, 9–11). Needless to say, earlier findings in which AF-2364 was used to identify the signaling pathways that regulate AJ dynamics in the testis could be the results of acute or chronic toxicity. We therefore sought to use another well characterized model, in which cell adhesion function between Sertoli cells and spermatids (step 8 and beyond) was compromised by intratesticular androgen suppression using testosterone-estradiol (TE) implants (for a review, see Ref. 12), to validate and expand these earlier observations. For instance, recent studies have shown that the loss of germ cells from the epithelium after AF-2364 treatment is regulated, at least in part, by a loss of protein-protein interactions in the ectoplasmic specialization (ES)-associated AJ-protein complexes, such as the cadherin-catenin complex (for a review, see Ref. 13). If such results can be reproduced in another *in vivo* model, this will undoubtedly eliminate the possibility that these earlier observations were artifacts of nonspecific drug effects. This would help to synthesize better compounds to perturb cell adhesion function conferred by these protein complexes, leading to the development of novel male pills.

Testosterone (T) is a male sex hormone that determines male phenotype and fertility. Its testicular level is approximately 100-fold of that in serum (14). A reduction of testicular T level by increasing serum T and estradiol-17β (E) levels in male rats using TE implants can suppress the development of step 8 spermatids and beyond, leading to their detachment from the epithelium possibly by compromising ES function (for reviews, see Refs. 12, 15). After TE implants are removed, and if rats are permitted to recover in the presence of excessive T or allowed to undergo spontaneous natural recovery (NR), a restoration of T level in the testes can be achieved, which is also accompanied by a reversal of spermatogenesis. Collectively, these observations illustrate that this is a novel model to study ES dynamics (for a review, see Ref. 12).

AQ: D

Myotubularin-related protein 2 (MTMR2) is a lipid phosphatase at 3D site within the myotubularin (MTM) family having a catalytic site found in protein tyrosine phosphatases (PTP) and dual specific phosphatases (16–18). Its mutation causes the demyelinating neuropathy Charcot-Marie-Tooth disease type 4B1 (CMT 4B1) (16, 19). MTMR2 dephosphorylates phosphatidylinositol 3-phosphate and phosphatidylinositol 3,5-bisphosphate, both *in vivo* and *in vitro*, and the product of the latter can act as a feedback regulator of MTMR2 (20, 21). Interestingly, MTMR2 is expressed by Sertoli and germ cells in the testis, and its level is induced during testicular maturation or when Sertoli-germ cell AJs are assembled *in vitro* (22, 23), implicating its role in AJ dynamics. A recent study has shown that MTMR2$^{-/-}$ mice displayed not only neuropathy but also azoospermia, accompanied by a significant reduction in testis size and weight, implicating the pivotal role of MTMR2 in AJ function and spermatogenesis (24). Besides forming homodimers between MTMR2 (25), MTMR2 can interact with several proteins in other epithelia such as MTMR5 (26). Moreover, neurofilament light chain protein and disc large 1 (Dlg1) are also structurally associated with MTMR2 in the brain (24, 27). However, a binding partner of MTMR2 has yet to be found in the testis. We therefore sought to identify the putative interacting partner(s) of MTMR2 in the seminiferous epithelium and to assess whether MTMR2 interacts with any protein kinases at the ES site to regulate cell adhesion function.

Materials and Methods

Animals

Male Sprague Dawley rats ranging between 20 and 90 d of age were obtained from Charles River Laboratories (Kingston, NY). Rats were killed by CO_2 asphyxiation. Testes were either removed immediately for testicular cell isolation or protein extraction or frozen for immunohistochemistry. The use of animals as reported herein was approved by The Rockefeller University Animal Care and Use Committee with Protocol Numbers 00111 and 03017.

Antibodies

Antibody against rat (r)MTMR2 was raised in a rabbit using a 22-amino-acid peptide (residues 156–177 of rMTMR2) of NH_2-TK*V*NERYELCD*T*YPALL*A*VPAN-COOH as earlier described (22), which shared 90.9% identity with human MTMR2 at residues 228–249 of NH_2-TK*I*NERYELCD*R*YPALL*V*VPAN-COOH. The italicized amino acids represent those that are different between the two species. Other antibodies used for immunoblotting studies are listed in Table 1.

AQ: E

T1

Isolation of seminiferous tubules

Seminiferous tubules isolated from 90-d-old rat testes with negligible Leydig cell contamination were obtained as described (28) and were used for lysate preparation.

Primary Sertoli cell cultures

Sertoli cells were isolated from 20-d-old rat testes as described (29). Cell number was determined by using a hemocytometer. Sertoli cells adjusted to the desired cell density were suspended in serum-free Ham's F12 nutrient mixture (F12) and DMEM (F12/DMEM, 1:1, vol/vol) supplemented with 15 mM HEPES, 1.2 g/liter sodium bicarbonate, 10 μg/ml bovine insulin, 5 μg/ml human transferrin, 2.5 ng/ml epidermal growth factor, 20 mg/liter gentamicin, and 10 μg/ml bacitracin. Twelve-well dishes were precoated with Matrigel (Collaborative Biochemical Products, Bedford, MA), diluted 1:6 (vol/vol) in F12/DMEM, and dried overnight at 35 C. Cells were plated on dishes at a density of 0.5×10^6 cell/cm^2 as described (30) with 3 ml F12/DMEM per well and incubated in a humidified atmosphere of 5% CO_2 and 95% air (vol/vol) at 35 C. Approximately 48 h after cell plating, Sertoli cells were hypotonically treated with 20 mM Tris (pH 7.4) to lyse residual germ cells (31), followed by two washes with F12/DMEM. The purity of Sertoli cells used for our studies was at least 95% as characterized by light and electron microscopy (32, 33).

TABLE 1. Antibodies used for immunoblotting experiments

Protein	Source	Catalog no.	Lot no.	Vendor
β-Actin	Goat	sc-1616	B1804	Santa Cruz Biotechnology
Axin	Rabbit	sc-14029	C012	Santa Cruz Biotechnology
α-Catenin	Rabbit	sc-7894	G3003	Santa Cruz Biotechnology
β1-Integrin	Mouse	610468	7	BD Transduction Lab
Laminin-γ3	Goat	sc-6601	B282	Santa Cruz Biotechnology
Phospho-Tyr	Rabbit	61-5800	40286685	Zymed Laboratories

balt3/zee-end/zee-end/zee00305/zee0730-05a | hurtr | S=12 | 1/21/05 | 7:52 | 4/Color Figure(s): 1,2,3,6,10 | Art: 1195093 | Input-lc

Sertoli-germ cell cocultures

Germ cells were isolated from 90-d-old rat testes by a mechanical procedure using sequential filtrations as described (34). For germ cell lysate preparation, cells were terminated within 3 h after their isolation. For cocultures, freshly isolated germ cells were suspended in F12/DMEM supplemented with 6 mM sodium lactate, 2 mM sodium pyruvate, 20 mg/liter gentamicin, and 10 μg/ml bacitracin. Cell number was determined by a hemocytometer. Germ cells at desired cell number were reconstituted in F12/DMEM in the absence or presence of T (2×10^{-8} or 2×10^{-7} M) (Sigma Chemical Co., St. Louis, MO) and cyproterone acetate (1×10^{-6} M) (Sigma). Germ cells were cocultured with Sertoli cells at a 1:1 ratio in which Sertoli cells had been cultured alone for 5 d at 0.5×10^6 cells/cm^2 forming an intact epithelium (33, 35). Cocultures were terminated at 24 and 48 h thereafter when functional anchoring junctions, such as desmosome-like junctions and apical ES, were formed (3, 36, 37).

Immunohistochemistry

Testes isolated from normal rats and from animals of different treatment groups were frozen immediately in liquid nitrogen. Frozen testes were embedded in OCT compounds (Miles Scientific, Elkhart, IN), and 8-μm sections were cut using a microtome in a cryostat at −20 C and mounted on poly-L-lysine-coated slides. Histostain-SP kits obtained from Zymed Laboratories (South San Francisco, CA) were used for immunohistochemistry as described (38, 39). Sections were air dried at room temperature, fixed in Bouin's fixative (4% formaldehyde in picric acid) for 5 min, and washed with PBS [10 mM sodium phosphate, 0.15 M sodium chloride (pH 7.4) at 22 C]. Sections were then treated with 3% hydrogen peroxide solution (vol/vol, in methanol) for 20 min to eliminate endogenous peroxidase activity and blocked with a serum blocking solution (10% nonimmune goat serum, Zymed). Rabbit anti-rMTMR2 serum (1:300, in 1% nonimmune goat serum) or preimmune rabbit serum (control, 1:300, in 1% nonimmune goat serum) was added onto sections, and slides were incubated in a humidified chamber at 35 C overnight. Thereafter, sections were rinsed in PBS and incubated with biotinylated goat antirabbit IgG for 30 min, to be followed by streptavidin peroxidase conjugate for 10 min. Color development was performed using aminoethylcarbazole mixture. Sections were counterstained using hematoxylin and mounted with Histomount (Zymed). All sections from different rats within an experimental group were processed simultaneously in two to three microscopic slides (with two to four sections per slide) to eliminate interexperimental variations. Micrographs were obtained using an Olympus DP70 12.5 MPa Digital Camera interfaced to an HP Vectra VL800 Workstation and the QCapture Suite V2.60 software package from Quantitative Imaging Corp. (Burnaby, Canada). Digital images were subsequently processed using Adobe Photoshop (version 7.0). All immunohistochemistry experiments were repeated at least eight to 12 times over a period of 10 months using either frozen or paraffin sections from different rats, and the results depicted in Figs. 1–3 are the representatives of these analyses.

Sample preparation and immunoblot analysis

Testicular cells, seminiferous tubules, testes, and brain previously trimmed into approximately 2 × 2-mm pieces, were sonicated for 15 sec in an immunoprecipitation (IP) buffer [0.125 M Tris, containing 0.15 M NaCl, 5 mM sodium chloromercuribenzoate, 2 mM EDTA, 2 mM *N*-ethylmaleimide, 2 mM phenylmethylsulfonyl fluoride, 5 μg/ml pepstatin A, 1% Nonidet P-40 (vol/vol), 10% glycerol (vol/vol) (pH 7.4) at 22 C] and centrifuged at 12,000 × *g* for 15 min to remove cell debris. The clear supernatant was designated cell/tissue lysates and stored at −80 C until used. Protein concentration was estimated by Coomassie blue dye-binding assay (40) using BSA as a standard. Equal amounts of protein (100 μg protein per lane) were resolved by SDS-PAGE onto 7.5% T SDS-polyacrylamide gels under reducing conditions as described (41). Proteins were electroblotted onto nitrocellulose membranes (0.45 μm, Schleicher and Schuell, Keene, NH). Target proteins in blots were detected by corresponding antibodies and visualized using an enhanced chemiluminescence kit (Amersham Pharmacia Biotech, Piscataway, NJ) as described (32, 38, 42). Each blot could be reused for up to five to six times with different primary antibodies after the initial primary and secondary antibodies were stripped using SDS as described (32, 43) without detectable protein loss when the level of β-actin was quantified at the beginning and the end of an experimental series.

Treatment of rats with AF-2364 to induce germ cell loss from the seminiferous epithelium

AF-2364 was synthesized as previously described (6) with a purity greater than 99.8% when examined by elemental analysis. Male rats [250–300 g body weight (BW)] were fed with a single dose of AF-2364 at 50 mg/kg BW as described (6, 7), which was shown to induce germ cell loss from the epithelium, in particular round, elongating, and elongated spermatids (44), by perturbing cell adhesion function in the epithelium (for reviews, see Refs. 2, 3). Rats at time 0 served as controls. Testes were removed at specific time points, frozen in liquid nitrogen, and stored at −80 C until used.

Induction of germ cell loss from the seminiferous epithelium using an in vivo androgen suppression model in adult rats with steroid implants

Ethyl vinyl acetate (DuPont ELVAX 770) implants (3 or 4 cm in length) filled with T (Sigma) and 0.4-cm implants filled with E (Sigma) were prepared as described (45). A single 3-cm T and a 0.4-cm E implant were placed under the skin along the dorsal surface of each male adult rat (n = 3 rats for each specified time point) to suppress the endogenous T level in the testis, which was shown to induce germ cell loss from the seminiferous epithelium (for reviews, see Refs. 12, 15). Rats were under anesthesia using ketamine HCl (~70 mg/kg BW) during the surgery. The surgical area (~2 cm^2) was shaved to remove hair, cleansed with 70% ethanol and Betadine (two times each). A small incision (~1.5 cm) was made using a sterile scalpel. Implants were carefully inserted under the skin, and the surgical site was stitched using Ethilon PC-S sterile, nonabsorbable surgical suture with a 19 PC prime needle (Ethicon Inc., Somerville, NJ). After 28 d, TE implants were removed from all rats under anesthesia as described above. In one group, rats (n = 3 rats for each time point) received four 4-cm T implants (without E) to permit rapid T recovery and resumption of spermatogenesis, whereas in the other group, rats were allowed to have spontaneous (*i.e.* natural) recovery without any steroid implants. Rats had free access to standard chow and water with a 12-h light, 12-h dark cycle. Rats at time 0 were designated controls. Testes were removed at specific time points, frozen in liquid nitrogen, and stored at −80 C until used.

AQ: F

Co-IP

Approximately 500 μg of protein from testis lysates, prepared as described above from normal rats, rats that underwent spontaneous recovery (NR) on d 42, or rats that received four 4-cm T implants to undergo rapid recovery on d 30, were used for IP. Samples were pretreated with 2 μg rabbit IgG (or mouse or goat IgG, depending on the source of the primary antibody) for 3 h, followed by an incubation with 10 μl protein A/G plus agarose (Santa Cruz Biotechnology, Santa Cruz, CA) to eliminate nonspecific interactions between lysates and IgG. After centrifugation at 1000 × *g* for 5 min to precipitate the IgG-nonspecifically bound protein complex, supernatants were collected for subsequent co-IP. In brief, 2 μg of an anti-rMTMR2 antibody, IgG against a target protein (*e.g.* c-Src), or normal rabbit IgG (negative control), was added and incubated with the supernatant at 4 C overnight. The immunocomplexes were then precipitated using 20 μl protein A/G plus agarose on a rotator (40 rpm) for 6 h. Immunoprecipitates were washed with 300 μl IP buffer (four times, by gentle resuspension of the pellet in the IP buffer followed by centrifugation at 1000 × *g* for 5 min). Proteins in the immunocomplexes were extracted in SDS-sample buffer [0.125 M Tris (pH 6.25) at 22 C containing 1% SDS (wt/vol), 1.6% 2-mercaptoethanol (vol/vol), and 20% glycerol (vol/vol)] at 100 C for 10 min, and samples were resolved by SDS-PAGE onto 7.5% *T* SDS-polyacrylamide gels. After proteins were electroblotted onto nitrocellulose papers, immunoblotting was performed as earlier described using different antibodies (38). Lysates from normal testes and seminiferous tubules served as positive controls to assess the specificity of the primary antibodies and the electrophoretic mobility of the target proteins.

balt3/zee-end/zee-end/zee00305/zee0730-05a | hurtr | S=12 | 1/21/05 | 7:52 | 4/Color Figure(s): 1,2,3,6,10 | Art: 1195093 | Input-lc

Immunofluorescence microscopy

Immunofluorescence microscopy was performed as earlier described (32, 46) to examine whether rMTMR2 and c-Src colocalized to the same site in the seminiferous epithelium, verifying results of IP that rMTMR2 and c-Src are indeed part of a structural complex at the ES. Frozen sections were fixed in Bouin's fixative (4% formaldehyde in picric acid) for 5 min and washed with PBS [10 mM sodium phosphate, 0.15 M sodium chloride (pH 7.4) at 22 C]. To eliminate interexperimental variation, all sections obtained from testes in different treatment groups within an experimental set were processed simultaneously in two slides because each slide holds at least three to four cross-sections of testes. This is necessary so that all sections within an experimental set can be stained, colorimetrically developed, and photographed simultaneously. Sections were blocked with 10% normal goat serum for 30 min. Sections were then incubated with a rMTMR2 antibody at a dilution of 1:200 in PBS containing 1% goat serum and then with a p-Src-Tyr^{416} antibody (Upstate AQ: G Biotechnology, Lake Placid, NY; catalog no. 05-677, lot 26419) at a concentration of 20 μg/ml in PBS containing 1% goat serum, to be followed by 1:50 fluorescein isothiocyanate (FITC) goat-antirabbit IgG conjugate (Zymed, catalog no. 62-6111, lot 30677924) and 1:50 goat antimouse IgG-CY3 conjugate (Zymed, catalog no. 81-6515, lot 31079880R). Sections were then mounted by using Vectashield mounting medium with 4′,6-diamidino-2-phenylindole (DAPI) (Vector Laboratories, Inc., Burlingame, CA; catalog no. H-1500, lot Q0220). Images were digitally captured by using an Olympus BX40 microscope with UPlanF1 fluorescent optics (Olympus Corp.) and an Olympus DP70 12.5 MPa digital camera. All data were analyzed using Adobe Photoshop (version 7.0). Controls included the use of either IgG or 1% goat serum instead of the primary antibodies, which failed to yield detectable fluorescence, illustrating that the staining was specific.

Statistical analysis

Statistical analysis was performed using the GB-STAT Statistical Analysis Software Package (version 7.0, Dynamic Microsystems, Inc., Silver Spring, MD).

Results

Immunohistochemical localization of rat MTMR2 (rMTMR2) in the rat testis

The immunohistochemical localization of rMTMR2 using a monospecific polyclonal antibody raised in rabbits is F1 shown in Fig. 1, A–H, which appeared as reddish-brown precipitates. Figure 1, B and C, are negative controls showing the staining with the preimmune serum. Figure 1C corresponds to the boxed area of Fig. 1B, illustrating that the staining shown in Fig. 1A was specific to rMTMR2. rMTMR2 was shown to associate with both Sertoli cells and germ cells in virtually all stages of the epithelial cycle (Fig. 1, A and D–H). However, rMTMR2 was detected predominantly at the site consistent with its localization at the apical ES at stages XI–IV of the epithelial cycle in the rat testis (Fig. 1, A and D–H). For instance, it localized to the heads of elongating spermatids at stage XII–IV at the apical ES (Fig. 1, D–H), as well as at the basal ES (Fig. 1, A and D–H). However, rMTMR2 was not detected at the apical ES at the Sertoli-elongating/elongate spermatid interface at stage V–VII, yet it became intensely localized to this site at stage VIII just before spermiation (Fig. 1F, compare the stage VIII tubule on the left and the stage V tubule on the right, *vs.* Fig. 1, A, D, E, G, and H). Furthermore, some staining of rMTMR2 was found in the interstitium, surrounding blood vessels. This latter finding suggests that rMTMR2 may also play a role in interstitial Leydig cells and blood vessel endothelium. These results are consistent with an earlier report, demonstrating

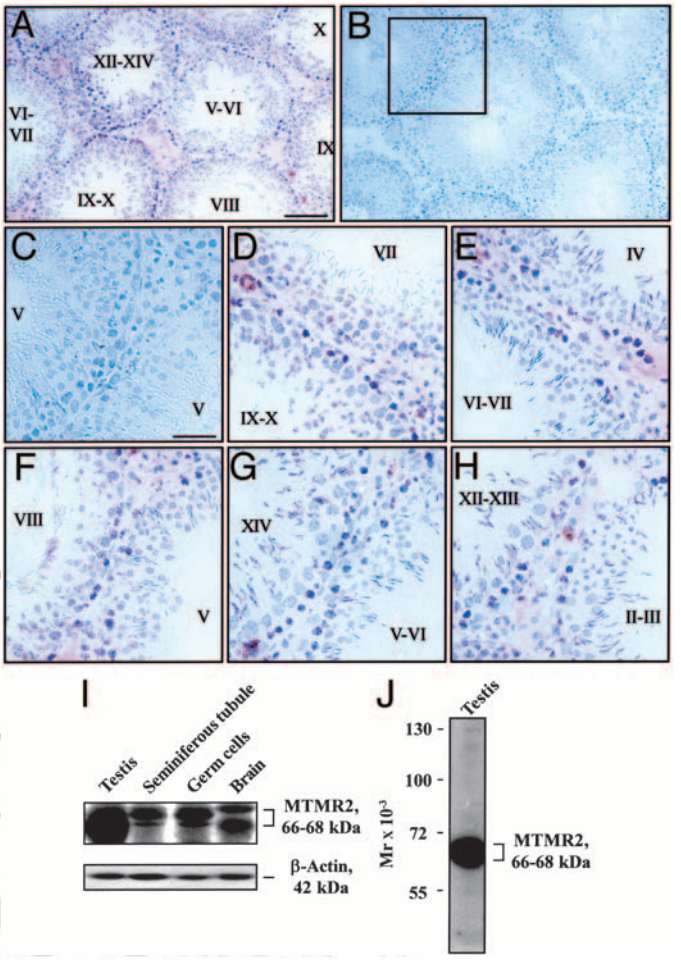

FIG. 1. Immunohistochemical localization of rMTMR2 in normal rat testes. Frozen sections obtained from testes of adult rats (~300 g BW) were immunostained for rMTMR2 using a rabbit anti-rMTMR2 polyclonal antibody (A, D–H) or with preimmune serum (B and C) as described in *Materials and Methods*. A and B, Corresponding low magnification of rat testes stained with the anti-rMTMR2 antibody (A) or preimmune serum (B). C–H, High magnification of testes showing tubules at different stages of the epithelial cycle. Immunoreactive rMTMR2 appear as *reddish-brown* precipitates. C, Corresponding magnified micrograph of the *boxed area* shown in B. rMTMR2 was localized to the Sertoli-spermatocyte interface at the basal compartment in the epithelium in virtually all stages of the epithelial cycle (D–H). rMTMR2 was also found to associate with elongating spermatids at stages XII-I at the apical ES site (G and H). In stages V-VII, however, rMTMR2 was associated mostly at the site of the basal ES but not apical ES. rMTMR2 was also predominantly localized at the Sertoli-elongate spermatid interface at stage VIII before spermiation at the site, consistent with its localization at the apical ES (F). *Bar*, 120 μm (A and B) and 40 μm (C and D–H). I, Immunoblot stained with the anti-rMTMR2 antibody illustrating the various isoforms of MTMR2 in lysates of testes, seminiferous tubules, and germ cells *vs.* the brain (~100 μg total protein per lane). The lower panel is the same blot as the upper panel but stained with an anti-β-actin antibody that served as the loading control. J, Immunoblot using testis lysates resolved on a 7.5% *T* SDS-polyacrylamide gel and stained with an anti-rMTMR2 antibody, demonstrating the specificity of this antibody.

rMTMR2 (formerly reported as rMTM) in round spermatids of stages VII and IX and Sertoli cells (22). Indeed, studies by immunoblotting using the lysates of testes, seminiferous tubules, germ cells, and brain (Fig. 1I) conclusively identified

balt3/zee-end/zee-end/zee00305/zee0730-05a | hurtr | S=12 | 1/21/05 | 7:52 | 4/Color Figure(s): 1,2,3,6,10 | Art: 1195093 | Input-lc

rMTMR2 in these tissues/cells that exists as three isoforms ranging between 66 and 68 kDa. Interestingly, germ cells were shown to produce rMTMR2 (Fig. 1I) consistent with the immunohistochemical data shown in Fig. 1, A–H. It is noted that these germ cells had negligible somatic cell contaminations when assessed by RT-PCR using primer pairs specific to protein markers of Leydig, peritubular myoid, and Sertoli cells (data not shown) as earlier reported (32, 43). The specificity of this antibody was also shown by immunoblot analysis (Fig. 1J).

Changes in the localization and protein level of rMTMR2 during AF-2364-induced AJ disruption in the seminiferous epithelium

AF-2364 (single dose, 50 mg/kg BW) was fed to adult rats at time 0 to induce germ cell depletion from the seminiferous epithelium by perturbing AJ function. Even before germ cell depletion was clearly visible in the epithelium, there was an increase in immunoreactive rMTMR2 in the epithelium, such as at the apical ES at the Sertoli-spermatid interface by d 1 after treatment compared with rats at time 0 (Fig. 2, A–C). When the event of germ cell depletion became more pronounced, more rMTMR2 was detected at the Sertoli-round spermatid interface (Fig. 2, D–G). A negative control using a preimmune serum is shown in Fig. 2H, illustrating the specificity of the rMTMR2 staining. Furthermore, these immunohistochemistry results were consistent with the immunoblot analysis shown in Fig. 2, I and J, when the rMTMR2 protein level was quantified in testis lysates. For instance, a surge of rMTMR2 was detected on d 1 after treatment (Fig. 2I). When more spermatids were being released to the lumen, the level of rMTMR2 also surged, increasing by almost 10-fold by d 15 after treatment when tubules were virtually devoid of germ cells except for some spermatogonia (Fig. 2, I, J, and G). By 60 d, when germ cells began to repopulate the epithelium (for reviews, see Refs. 2, 6), the rMTMR2 protein level also subsided (Fig. 2I), illustrating that the resumption of spermatogenesis and possibly AJ recovery are associated with a tumbling of rMTMR2. Figure 2I, *bottom*, shows an anti-β-actin staining using the same blot as the *top*, which served as the protein loading control.

Changes in the localization and protein level of rMTMR2 in the rat testis during androgen suppression-induced AJ disruption and its recovery

When a 3-cm T and a 0.4-cm E implant were inserted into adult rats at time 0 to suppress the endogenous T level in the testis, this procedure would induce AJ disruption and germ cell loss from the seminiferous epithelium (12, 15, 47). On d 28, both implants were removed and four 4-cm T implants were inserted to the same site in half of the rats (n = 3 for each time point) to induce rapid recovery of androgen level,

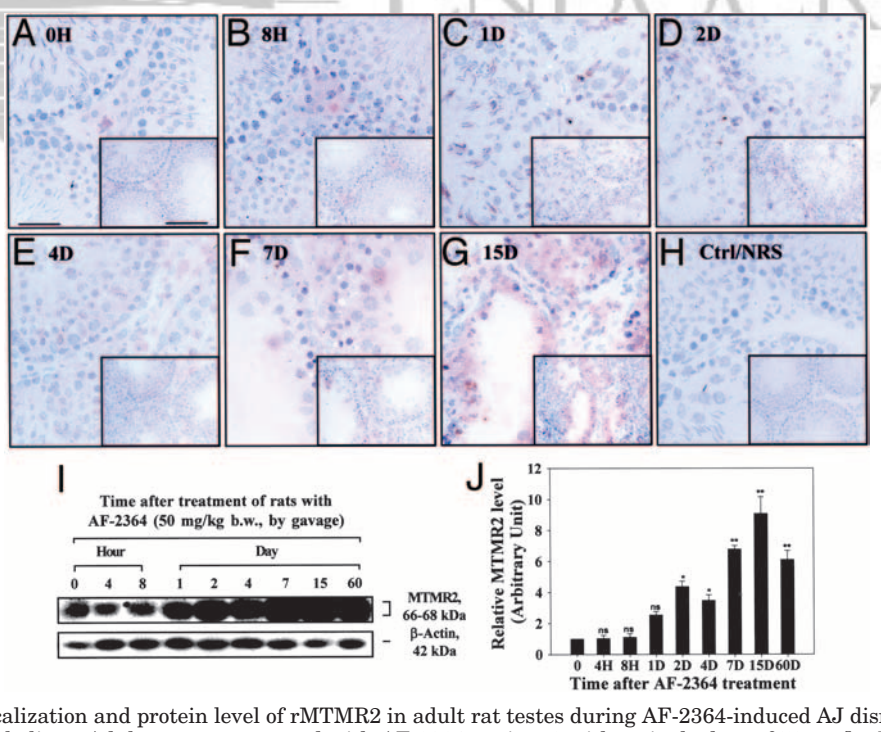

FIG. 2. Changes in the localization and protein level of rMTMR2 in adult rat testes during AF-2364-induced AJ disruption and germ cell loss from the seminiferous epithelium. Adult rats were treated with AF-2364 at time 0 with a single dose of 50 mg/kg BW by gavage, and testes were removed at specific time points. Frozen cross-sections were prepared for immunohistochemical staining with a rabbit anti-rMTMR2 serum (A–G) or with a preimmune rabbit serum (H). An increase in rMTMR2 staining became clearly visible between d 1 and 15 after AF-2364 treatment (C–G *vs.* A and B). *Bar* in A, 40 μm, which applies to B–H; *bar* in *inset* of A, 150 μm, which applies to *insets* in B–H. I, An immunoblot that used lysates of testes (100 μg total protein per lane) from rats treated with AF-2364, showing an increase in rMTMR2 protein level during AF-2364-induced AJ disruption, which was visible within 1 d after treatment. This increase persisted until d 15 when almost all spermatids had depleted from the seminiferous epithelium (F and G). A mild decline in MTMR2 protein level was detected at 60 d after AF-2364 treatment. The *bottom* panel of I is an anti-β-actin staining using the same blot as the *top* panel that served as the loading control. J, Densitometrically scanned data using fluorograms such as the one shown in I but normalized against β-actin protein levels (n = 3). ns, Not significantly different from 0 h by Student's *t* test; *, significantly different at $P < 0.05$; **, significantly different at $P < 0.01$.

balt3/zee-end/zee-end/zee00305/zee0730-05a | hurtr | S=12 | 1/21/05 | 7:52 | 4/Color Figure(s): 1,2,3,6,10 | Art: 1195093 | Input-lc

whereas the other half of the animals (n = 3 per time point) were allowed to undergo spontaneous recovery (NR) without any steroid implants (for a review, see Ref. 12). Similar to the AF-2364 model, there was a progressive surge in rMTMR2 staining in the epithelium during androgen suppression-induced germ cell loss (Fig. 3, C and D *vs.* A and B). For instance, when most of the tubules were still devoid of elongating/elongate spermatids by d 42 (note that TE implants were removed on d 28) and permitted to undergo spontaneous recovery, the staining of rMTMR2 was very

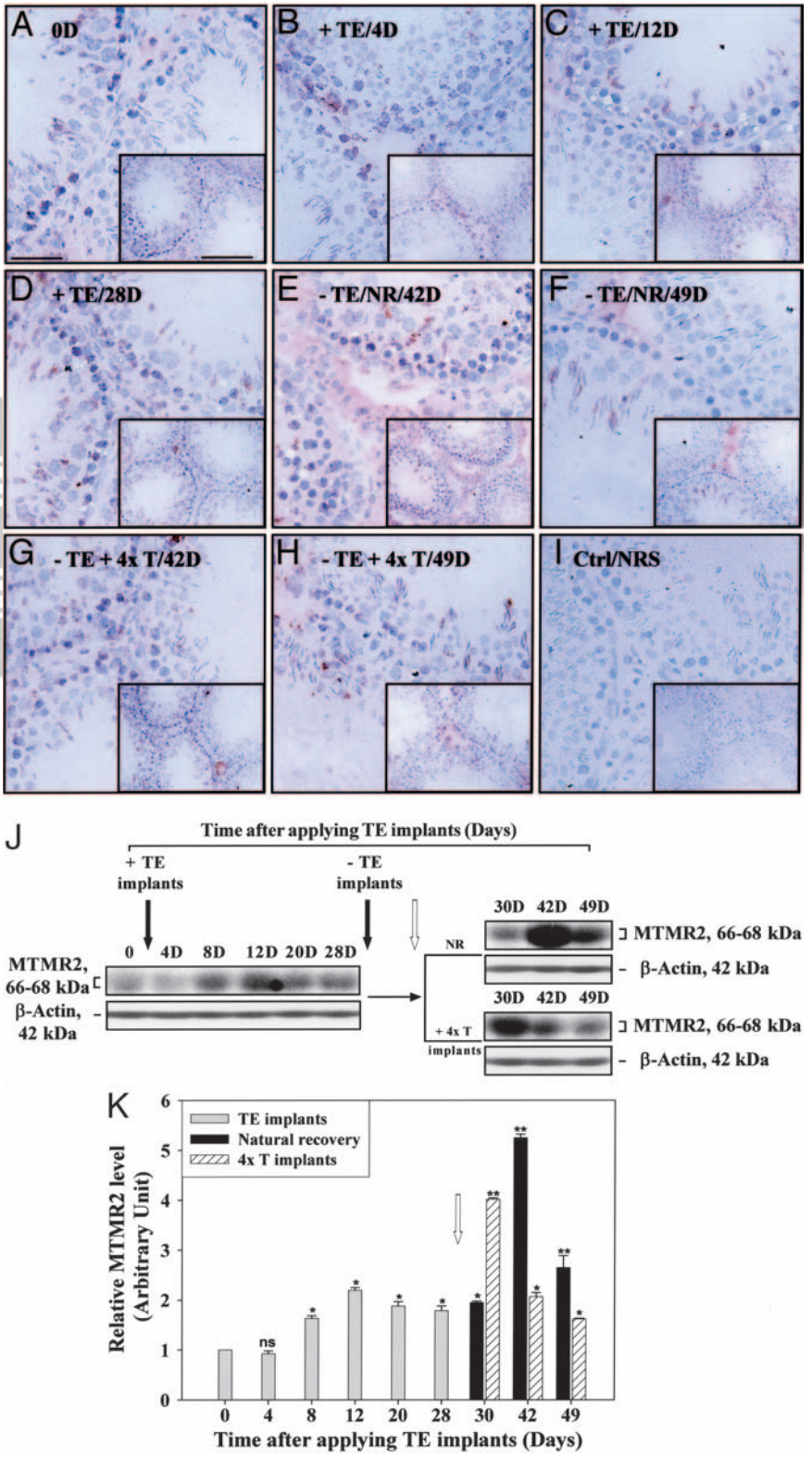

FIG. 3. Changes in the localization and protein level of rMTMR2 in the rat testis during androgen suppression-induced (TE implants) germ cell loss and AJ disruption, its NR, and high-dose-T-induced recovery (four T implants). Adult rats were treated with one T (3-cm) and one E (0.4-cm) (TE) implant inserted under the skin at the dorsal surface. After 28 d, TE implants were removed and replaced by four T implants (each was 4-cm long) or rats were allowed to undergo spontaneous natural recovery (NR) without any implants. Frozen cross-sections were prepared for staining with rabbit anti-rMTMR2 serum (A–H) or with preimmune rabbit serum (I). *Bar* in A, 40 μm, which applies to B–I. rMTMR2 appeared as reddish brown precipitates in the seminiferous epithelium. *Bar* in *inset* of A, 150 μm, which applies to *insets* in B–I. J, An immunoblot using lysates of testes showing changes in rMTMR2 protein level during TE-induced AJ disruption and during spontaneous recovery or high-androgen-level-induced recovery with T implants. The *bottom* panel shows the same blot as the *top* panel but stained with an anti-β-actin antibody and served as a protein loading control. K, Densitometrically scanned data using fluorograms, such as those shown in J but normalized against β-actin to account for uneven protein loading (n = 3). ns, not significantly different from 0 h by Student's *t* test; *, significantly different at $P < 0.05$; **, significantly different at $P < 0.01$. The *open arrow* shown in panels J and K indicates rats were allowed to undergo either NR or received four T implants (each was 4-cm in length), which is applicable to other figures in this report.

balt3/zee-end/zee-end/zee00305/zee0730-05a | hurtr | S=12 | 1/21/05 | 7:52 | 4/Color Figure(s): 1,2,3,6,10 | Art: 1195093 | Input-lc

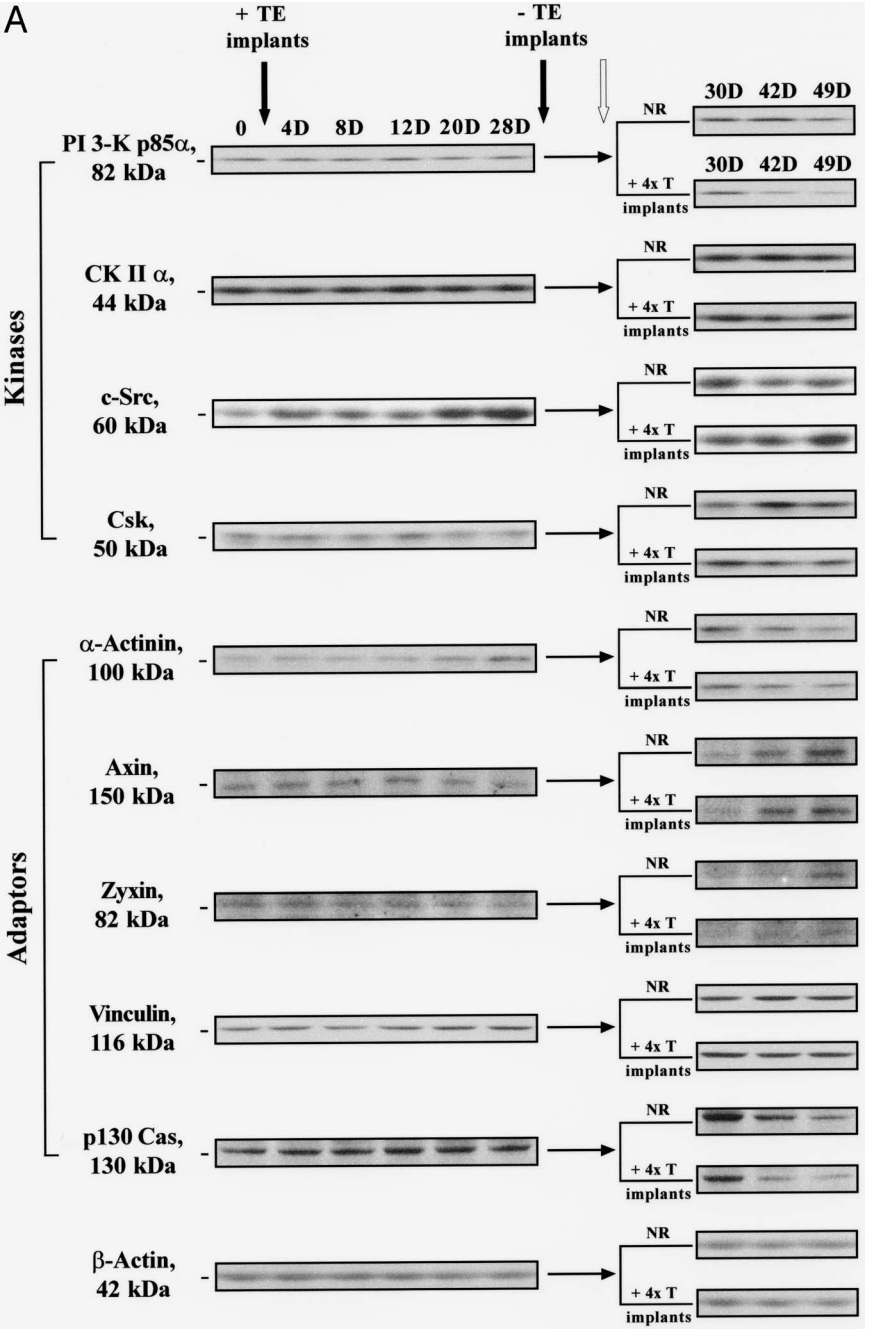

FIG. 4. Changes in the protein levels of selected kinases and adaptors in the rat testis during androgen suppression-induced germ cell loss and AJ disruption, its spontaneous natural recovery, and high-dose-T-induced recovery. A, Immunoblot analysis using lysates of testes showing changes in the protein levels of kinases (PI 3-K p85α, CK IIα, c-Src, and Csk) and adaptors (α-actinin, axin, zyxin, vinculin, and p130Cas) during androgen depletion-induced germ cell depletion and its recoveries. These target proteins were recently identified at the Sertoli-germ cell ES site (see text for references). The *bottom panel* shows a blot stained with an anti-β-actin antibody and served as a protein loading control. B, Densitometrically scanned data (a–i) using fluorograms, such as those shown in A, but normalized against β-actin to account for uneven protein loading (n = 3). ns, Not significantly different from 0 h by Student's *t* test; *, significantly different at $P < 0.05$; **, significantly different at $P < 0.01$.

intense in the epithelium (Fig. 3E), yet rMTMR2 staining was greatly reduced when spermatids began to reappear in the epithelium in rats that either received four T implants or underwent NR (Fig. 3, F–H *vs.* E). Based on the observation of such a rapid recovery of spermatids in the epithelium, within approximately 20 d, it is logical to conclude that most spermatocytes were not depleted from the epithelium by this treatment. Figure 3I shows a normal testis stained with preimmune rabbit serum that served as a negative control. Such changes in immunohistochemical localization of rMTMR2 during androgen suppression-induced spermatid loss and the subsequent recovery were verified by immunoblotting shown in Fig. 3, J and K. For instance, rMTMR2 was induced by d 8 after receiving TE implants and reached its peak by 42 d in the NR group but peaked by 30 d in the four-T-implants group and declined gradually during the recovery phase. The lower panels of Fig. 3J are the same blots as the upper panels but stained with an anti-β-actin antibody to illustrate equal protein loading.

Effects of androgen suppression-induced AJ disruption and its recovery on the protein levels of selected kinases and adaptors in the seminiferous epithelium in vivo

To investigate possible MTMR2 interacting protein partners, including kinases and adaptors, immunoblot analysis

balt3/zee-end/zee-end/zee00305/zee0730-05a | hurtr | S=12 | 1/21/05 | 7:52 | 4/Color Figure(s): 1,2,3,6,10 | Art: 1195093 | Input-lc

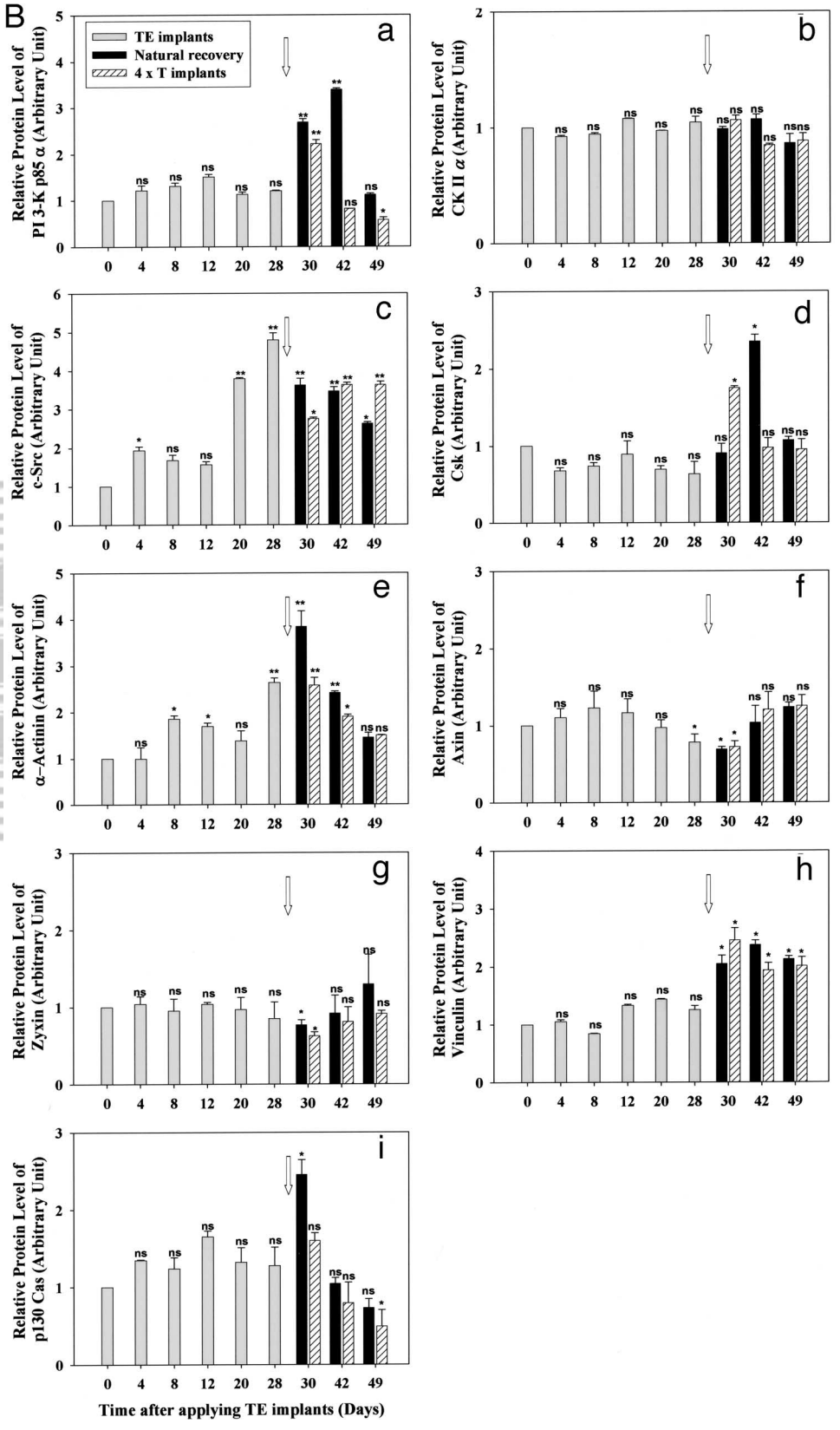

FIG. 4. *Continued*

was first performed to assess whether any signaling proteins/adaptors were induced. As shown in Fig. 4, A and B, an increase in protein levels were found for phosphatidylinositol 3-kinase (PI 3-K) p85α, c-Src, C-terminal Src kinase (Csk), α-actinin, vinculin, and p130Cas, whereas no significant changes were detected for casein kinase (CK) IIα, axin,

balt3/zee-end/zee-end/zee00305/zee0730-05a | hurtr | S=12 | 1/21/05 | 7:52 | 4/Color Figure(s): 1,2,3,6,10 | Art: 1195093 | Input-lc

and zyxin during androgen-induced AJ disruption. PI 3-K p85α, Csk, and vinculin displayed a similar trend; their protein levels were induced before the epithelium was fully recovered naturally on d 42 and on d 30 in the high-dose T recovery group, but tumbled thereafter (Fig. 4, A and B), which was somewhat later than MTMR2 (Fig. 3J). c-Src, α-actinin, and p130Cas were also induced, yet their induction was detected earlier, such as by d 20–28 after TE implants were placed to deplete androgen, and their recoveries were also earlier (Fig. 4, A and B), similar to MTMR2 (Fig. 3J). These findings suggest that the expression of these two groups of proteins may be regulated differently at the time of androgen depletion-induced germ cell loss and its recoveries. The *bottom panel* in Fig. 4A is the corresponding blot stained for β-actin to illustrate equal protein loading.

rMTMR2 is structurally associated with c-Src in the seminiferous epithelium during androgen suppression-induced germ cell loss

Co-IP was performed to identify the interacting partner(s) of MTMR2 by screening the kinases and adaptors that were recently found in the rat testis (13, 43) using testis lysates from samples of the androgen depletion model. It was shown that c-Src (Fig. 5A), but neither PI 3-K p85α nor vinculin (Fig. 5, B and C), was associated with MTMR2. All other kinases and adaptors that were examined also failed to associate with MTMR2 (Fig. 5D). F5

Colocalization of rMTMR2 with p-Src-Tyr^{416} in the rat testis

To verify results of the co-IP experiment that rMTMR2 indeed structurally interacted with c-Src, a study using immunofluorescent microscopy was performed. Figure 6 illustrates the colocalization pattern of rMTMR2 and p-Src-Tyr^{416}, the active form of c-Src, in a stage VIII tubule. rMTMR2 appeared as green fluorescence with an FITC conjugate (Fig. 6A). p-Src-Tyr^{416} appeared as red fluorescence with a Cy3 conjugate (Fig. 6B). It is apparent that p-Src-Tyr^{416} has a more restricted distribution in the epithelium and was confined to the apical ES. This is somewhat different from c-Src because c-Src was localized both at the apical ES as well as at the interface of Sertoli cell and round spermatids/spermatocytes F6

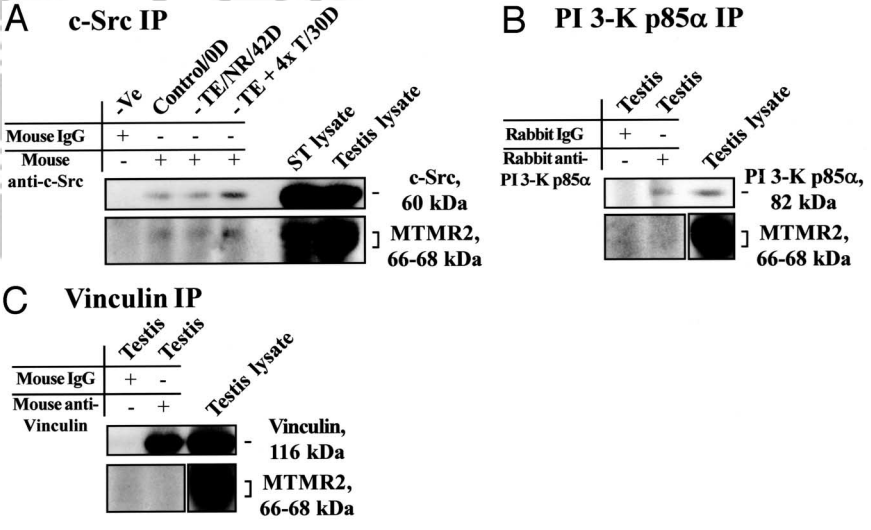

FIG. 5. A study using co-IP to assess the association between rMTMR2 and different kinases and adaptors in rat testes during androgen depletion-induced germ cell loss from the seminiferous epithelium. Approximately 500 μg protein of lysates from untreated rat testes, from spontaneous natural recovery on d 42, and from high-dose-T recovery on d 30 were used for co-IP using different antibodies (A, anti-c-Src; B, anti-PI 3-K p38α; C, anti-vinculin) as described in *Materials and Methods*. The immunocomplexes were precipitated using protein A/G plus agarose, extracted in SDS-sample buffer, and resolved by SDS-PAGE onto 7.5% T SDS-polyacrylamide gels. After proteins were electroblotted onto nitrocellulose papers, blots were incubated with either an anti-rMTMR2 antibody or an antibody against a target protein. Igs of the corresponding animal species were used for negative controls depending on the source of the primary antibody. Lysates of normal rat testes and seminiferous tubules (ST lysate) were used as positive controls, illustrating the antibody specificity. rMTMR2 was found to structurally associate with c-Src but not other proteins examined. PI 3-K p85α and vinculin, which failed to associate with rMTMR2, were also shown. D, Tabulated co-IP results using different antibodies on proteins found at the ES site. +, positive co-IP result; –, negative result.

D Association of MTMR2 with other proteins examined by Co-IP

	Proteins	Source	Cat. no.	Lot no.	Vendor	MTMR2
Kinases:	PI 3-K p85α	Rabbit	06-497	25086	Upstate	-
	c-Src	Mouse	sc-8056	J2103	Santa Cruz	+
	CK II α	Rabbit	sc-9030	B221	Santa Cruz	-
	Csk	Rabbit	sc-286	E091	Santa Cruz	-
	FAK	Rabbit	sc-558	D1204	Santa Cruz	-
	p-FAK-Tyr^{397}	Rabbit	07-012	23319	Upstate	-
Adaptors:	α-Actinin	Goat	sc-7453	D292	Santa Cruz	-
	p130 Cas	Rabbit	06-500	19950	Upstate	-
	Vinculin	Mouse	V9131	70K4877	Sigma	-
	ZO-1	Rabbit	61-7300	40588002	Zymed	-
	Zyxin	Goat	sc-6438	E138	Santa Cruz	-
AJ proteins:	Afadin	Rabbit	A0349	012K4875	Sigma	-
	N-Cadherin	Rabbit	sc-7939	J1502	Santa Cruz	-
	β-Catenin	Rabbit	sc-7199	L0203	Santa Cruz	-
	Nectin 3	Goat	sc-14805	D102	Santa Cruz	-

* -, no association; +, positive association

balt3/zee-end/zee-end/zee00305/zee0730-05a | hurtr | S=12 | 1/21/05 | 7:52 | 4/Color Figure(s): 1,2,3,6,10 | Art: 1195093 | Input-lc

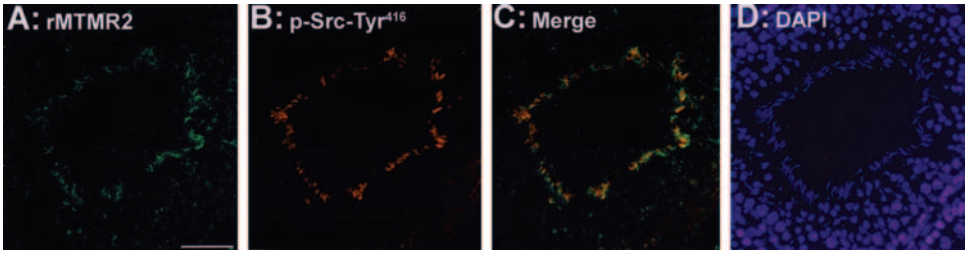

FIG. 6. A study using immunofluorescent microscopy to colocalize rMTMR2 with p-Src-Tyr^{416} in the seminiferous epithelium of adult rat testes. A, Immunofluorescent micrograph showing the localization of rMTMR2 in the seminiferous epithelium of a stage VIII tubule using a rabbit polyclonal anti-rMTMR2 antibody. The second antibody was an FITC goat antirabbit IgG conjugate. B, The corresponding immunofluorescent micrograph showing p-Src-Tyr^{416} using a mouse anti-p-Src-Tyr^{416} antibody and a goat antimouse IgG-CY3 conjugate. C, Merged image of A and B for rMTMR2 and p-Src-Tyr^{416}, respectively, showing rMTMR2 and p-Src-Tyr^{416} were colocalized to the apical ES site in the seminiferous epithelium. D, DNA staining with DAPI, illustrating this is a stage VIII tubule. *Bar* in A, 40 μm, which applies to B–D.

at stages VI–VIII as recently reported (13). The merged image of Fig. 6, A and B, is shown in Fig. 6C, illustrating rMTMR2 and p-Src-Tyr^{416} were indeed colocalized to the same site at the apical ES. Figure 6D is a DAPI staining.

Effects of androgen suppression-induced AJ disruption and its recovery on the protein levels of AJ structural protein complexes N-cadherin/β-catenin, β1-integrin/laminin-γ3, and nectin 3/afadin in the rat testis

To further identify the AJ structured proteins that are the possible substrates of MTMR2 and c-Src, we have also investigated the changes in protein levels of three known structural protein complexes at the apical ES, namely N-cadherin/β-catenin, β1-integrin/laminin-γ3, and nectin 3/afadin, using testis lysates from the androgen depletion model (Fig. 7A). N-Cadherin, β-catenin, β1-integrin, and afadin were all induced during androgen suppression-induced germ cell loss, whereas nectin 3 was reduced and laminin-γ3 displayed no significant change. Except for laminin-γ3, all other structural proteins began to recover in 2 d after TE implants removal (*i.e.* d 30 after rats had received TE implants that were removed on d 28). This pattern of changes in AJ structural protein complexes illustrates that many AJ proteins were induced during germ cell loss, possibly trying to rescue the epithelium, and they returned to their normal levels during recovery. A representative β-actin blot was also shown in the lower panel to verify equal protein loading.

Changes in the protein levels of rMTMR2, c-Src, and α-catenin in Sertoli-germ cell cocultures with and without treatments with T or cyproterone acetate (CPA) plus T

The data shown above seemingly suggest that rMTMR2 and c-Src are regulated, at least in part, by T, and because c-Src has recently been shown to associate with the cadherin/catenin protein complex, we had used an *in vitro* model of Sertoli-germ cell cocultures to examine the effects of androgens on these proteins. Sertoli cells were cultured alone for 5 d to permit Sertoli-Sertoli AJ and tight junction assembly, forming an intact cell epithelium (33). On d 6, germ cells were isolated from adult rat testes and added onto the Sertoli cell epithelium to initiate Sertoli-germ cell AJ assembly because functional ES and desmosome-like junctions are known to form within 24–48 h, as earlier described from this laboratory (3, 36), in the presence or absence of either T or CPA (an antiandrogen) plus T. This experiment was used to assess the effects of T or T plus CPA on protein levels of MTMR2 and c-Src during AJ assembly *in vitro* (Fig. 8A). It was shown that

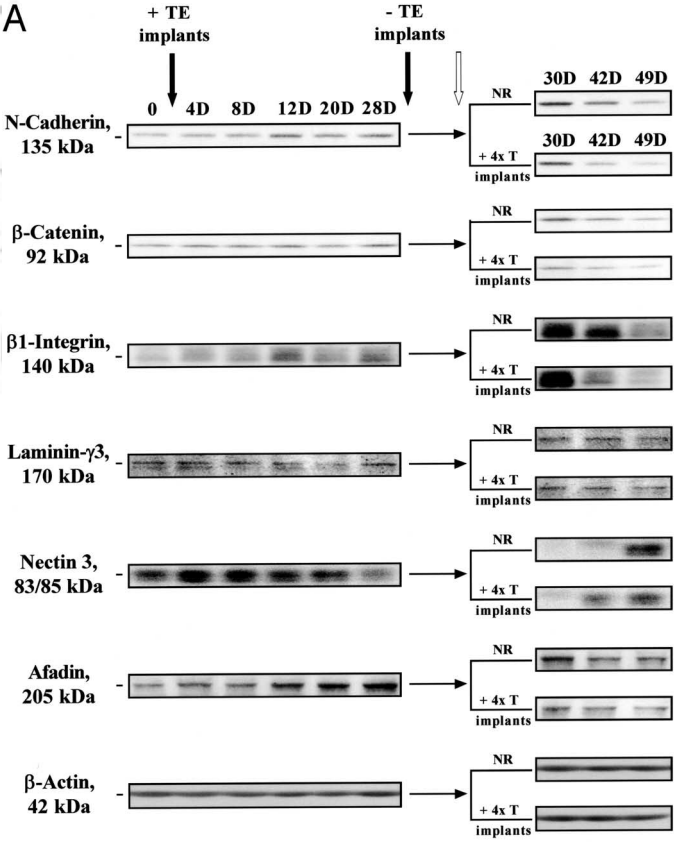

FIG. 7. Changes in the levels of AJ structural protein complexes N-cadherin/β-catenin, β1-integrin/laminin-γ3, and nectin3/afadin in the rat testis during androgen depletion-induced germ cell loss, its spontaneous natural recovery, and T-induced recovery. A, Immunoblot analysis using testis lysates showing changes in the protein levels of N-cadherin, β-catenin, β1-integrin, laminin-γ3, nectin3, and afadin during androgen-induced germ cell depletion and its recovery. The *bottom* panel shows the same blot as the *top* panel but stained with an anti-β-actin antibody and served as a protein loading control. B, Densitometrically scanned data (a–f), using fluorograms, such as those shown in A but normalized against β-actin to account for uneven protein loading (n = 3). ns, not significantly different from 0 h by Student's *t* test; *, significantly different at $P < 0.05$; **, significantly different at $P < 0.01$.

balt3/zee-end/zee-end/zee00305/zee0730-05a | hurtr | S=12 | 1/21/05 | 7:52 | 4/Color Figure(s): 1,2,3,6,10 | Art: 1195093 | Input-lc

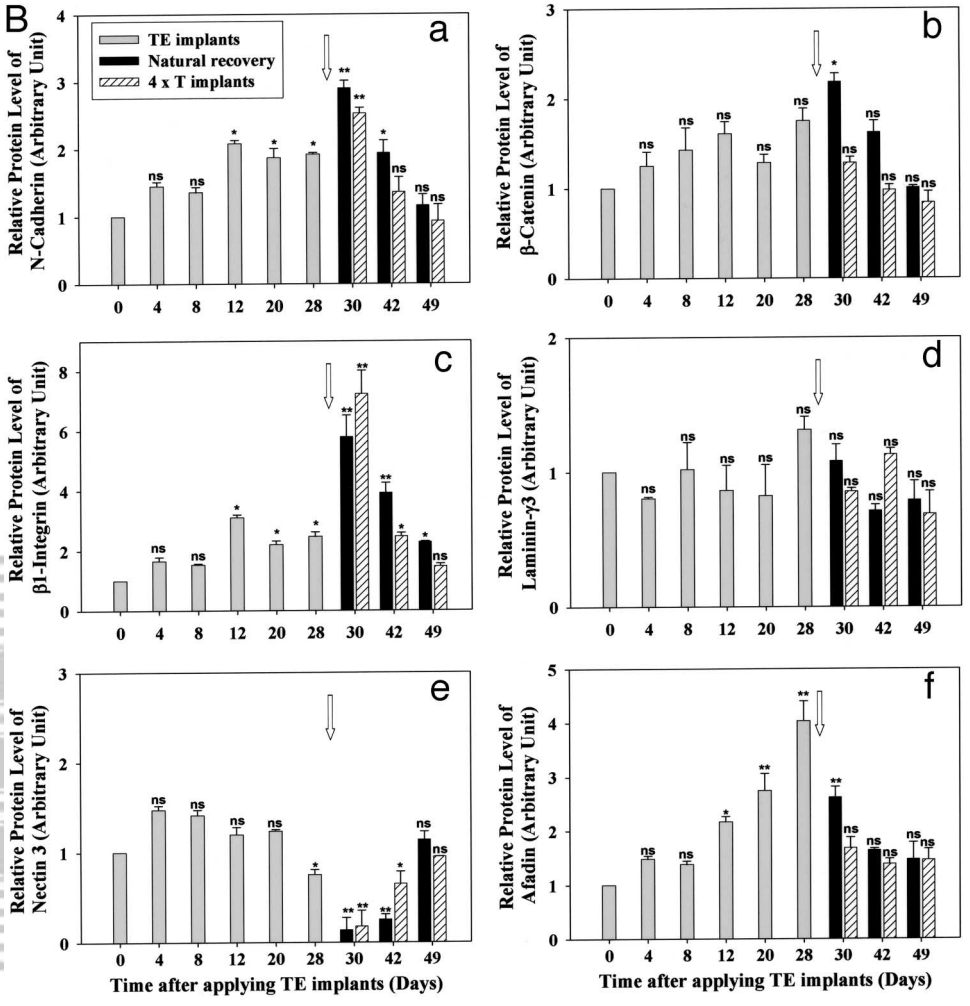

FIG. 7. *Continued*

the levels of both MTMR2 and c-Src were induced when cocultures were treated with either 0.02 or 0.2 μM T (the latter represents the normal intratesticular T level) (14). More importantly, this androgen-induced MTMR2 and c-Src protein productions were blocked by CPA (Fig. 8, A and B), illustrating the specificity of the androgen treatment. Because α-catenin was shown to be T inducible and c-Src was known to bind to the cadherin/catenin complex via catenin (13), the corresponding α-catenin blot served as an internal positive control. Indeed, α-catenin was induced by T treatment in cocultures and such induction could be blocked by CPA (Fig. 8, A and B). The *bottom panel* was the same blot as the *upper panels* but reprobed with an anti-β-actin antibody that served as a protein loading control.

The loss of protein-protein interactions in the N-cadherin/β-catenin protein complex with a concomitant increase in β-catenin Tyr phosphorylation during androgen suppression-induced germ cell loss from the seminiferous epithelium

Co-IP was performed using testis lysates from selected samples to identify any changes in protein-protein interactions in the N-cadherin/β-catenin protein complex. This complex was selected because earlier studies have demonstrated that c-Src, the binding partner of MTMR2, is structurally associated with catenins (13). As shown in Fig. 9, A and B, there was a significant loss in the interactions between N-cadherin and β-catenin (Fig. 9, A–C) regardless of whether co-IP was performed using an anti-cadherin or an anti-catenin antibody during androgen suppression-induced germ cell loss from the epithelium. This effect appears to be specific because when spermatids reattached to the epithelium during the recovery phase, the interactions between cadherins and catenins were reestablished, making them indistinguishable from normal testes (Fig. 9, A–C). More important, it was shown that when β-catenin lost its ability to associate with N-cadherin during androgen suppression-induced germ cell loss, the Tyr-phosphorylation status of β-catenin was significantly increased. However, when the cadherin-catenin interaction was reestablished during the recovery phase, the induced Tyr phosphorylation of β-catenin subsided (Fig. 9, B and C). Interestingly, when co-IP was performed using a c-Src antibody and the resultant blot was probed with an anti-β-catenin antibody, we also detected a loss of c-Src association with β-catenin during germ cell loss (Fig. 9, B and C). And more c-Src was found to reassociate with β-catenin during the recovery (Fig. 9B). Based on the findings reported herein, we now propose a molecular model that illustrates

balt3/zee-end/zee-end/zee00305/zee0730-05a | hurtr | S=12 | 1/21/05 | 7:52 | 4/Color Figure(s): 1,2,3,6,10 | Art: 1195093 | Input-lc

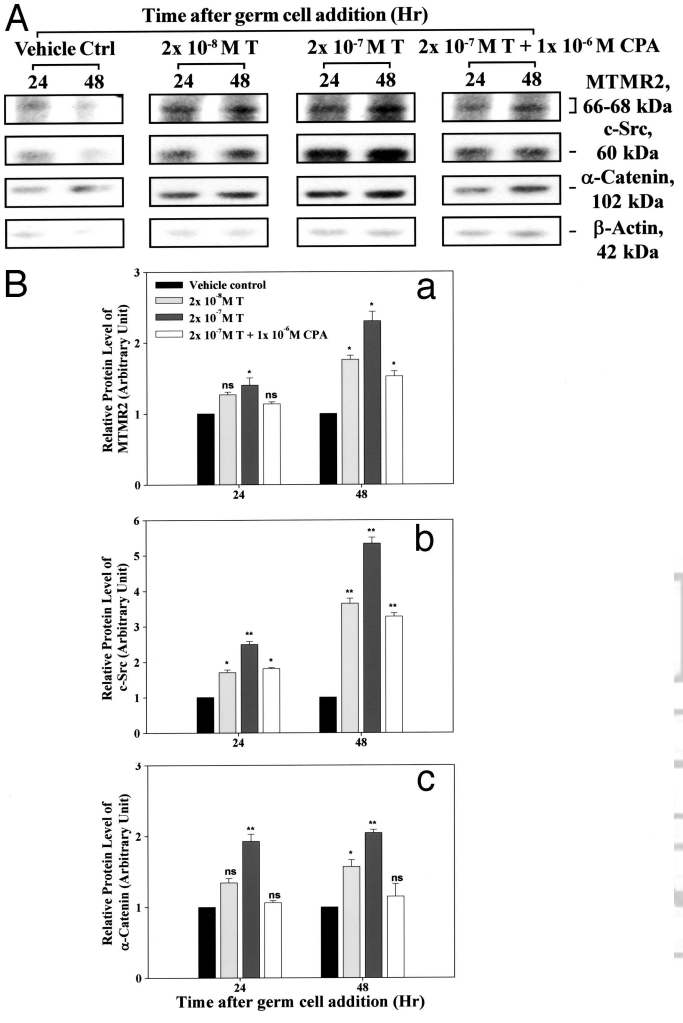

FIG. 8. A study to assess the effects of T on the expression of MTMR2, c-Src, and α-catenin during Sertoli-germ cell AJ assembly. A, Changes in the protein levels of rMTMR2, c-Src, and α-catenin in Sertoli-germ cell cocultures with and without treatments with T or T plus CPA were quantified by immunoblotting. Sertoli cells were isolated and cultured alone for 5 d, forming an intact cell epithelium. On d 6, germ cells were isolated from adult rat testes and added onto the Sertoli cell epithelium to initiate AJ assembly with or without T or T plus CPA as described in *Materials and Methods*. Cocultures were terminated at specified time points, and cell lysates were prepared for immunoblotting using antibodies against rMTMR2, c-Src, and α-catenin. The *bottom* panel is the same blot as the upper panel but stained with an anti-β-actin antibody and served as a protein loading control. The production of rMTMR2, c-Src, and α-catenin in these cocultures were stimulated by T. This stimulatory effect appears to be specific because the use of an anti-androgen, CPA, could block the T-induced protein production. B, The histograms shown in a–c correspond to the relative protein levels of MTMR2, c-Src, and α-catenin, respectively, after densitometric scanning using blots such as those shown in A but normalized against β-actin with n = 3 from three separate experiments during different cell preparations. The level of a target protein at 24 h (Hr) for vehicle control was arbitrarily set at 1. ns, not significantly different from vehicle control at 24 h by Student's *t* test; *, significantly different at $P < 0.05$; **, significantly different at $P < 0.01$.

the significance of T on the integrity of the cadherin-catenin protein complex at the ES site. Although an increase or a decrease in endogenous T can induce the production of N-cadherin, β-catenins, cSrc, and MTMR2 (Fig. 10) as reported herein, the integrity of the cadherin/catenin complex is compromised when the T level is suppressed because of a loss of protein-protein interactions between N-cadherin and β-catenin, as well as between β-catenin and cSrc, as illustrated in Fig. 10. An increase in T not only induces the production of N-cadherin, β-catenin, MTMR2, and c-Src proteins, but it also stabilizes protein-protein interactions between these proteins at the ES site (Fig. 10). F10

Discussion

Is the loss of cell adhesion function during androgen suppression-induced germ cell loss mediated by similar mechanism(s) found in the AF-2364 model?

AF-2364 is an analog of lonidamine [1-(2,4-dichlorobenzyl)-indazole-3-carboxylic acid] (6), which is a nonhormonal and nonsteroidal anticancer drug used in chemotherapy (for a review, see Ref. 5). Earlier studies have shown that AF-2364 can activate the transient expression of testin, an ES-associated signaling molecule, and was accompanied by germ cell depletion from the seminiferous epithelium possibly via a loss of AJ function at the Sertoli-germ cell interface, rather than a direct toxic effect on germ cells. This conclusion was reached because the antifertility effect of AF-2364 was not detectable by mating studies until almost 20–30 d after treatment after the sperm reserve in the epididymis was exhausted (6, 7). Furthermore, there is no specific organ uptake because the level of [^{3}H]AF-2364 found in the testis, the epididymis, and virtually all other organs examined after a single oral dose of approximately 22 μCi [^{3}H]AF-2364 was similar (for a review, see Ref. 8). If AF-2364 were toxic to germ cells, its antifertility effects would have been detected much sooner than 20–30 d after treatment (for a review, see Ref. 2). In a preliminary kinetics study, after a single dose of AF-2364 (50 mg/kg BW, by gavage) in adult rats, it was reported that elongating/elongate spermatids but not spermatocytes and spermatogonia began to deplete from the epithelium within 6–12 h (44). Greater than 95% of tubules examined became devoid of spermatids and spermatocytes by 28–79 d, yet germ cells began to repopulate the epithelium by d 128. Tubules fully recovered by d 210–254, and the morphology of the epithelium was indistinguishable from that of normal rats when examined histologically (6), suggesting that the effects of AF-2364 were reversible. Recent studies by electron microscopy have also illustrated that AF-2364 exerts its effect at the Sertoli cell-spermatid and the Sertoli cell-spermatocyte AJ site without affecting the Sertoli cell-spermatogonium interface (4, 43). Ongoing toxicity studies have also indicated that AF-2364 is neither nephrotoxic nor hepatotoxic at doses that are effective to induce transient infertility in male rats (for a review, see Ref. 2). Recent studies have shown that the AF-2364-induced germ cell loss is mediated, at least in part, by a loss of protein-protein interactions of the ES-structural protein complexes at the Sertoli-spermatid interface, such as between N-cadherin and β-catenin (13). To further confirm that protein-protein interactions are crucial to cell adhesion function in the epithelium and that this earlier observation is not the result of nonspecific interactions between AF-2364 and the cadherin/catenin protein complex, we have thus

balt3/zee-end/zee-end/zee00305/zee0730-05a | hurtr | S=12 | 1/21/05 | 7:52 | 4/Color Figure(s): 1,2,3,6,10 | Art: 1195093 | Input-lc

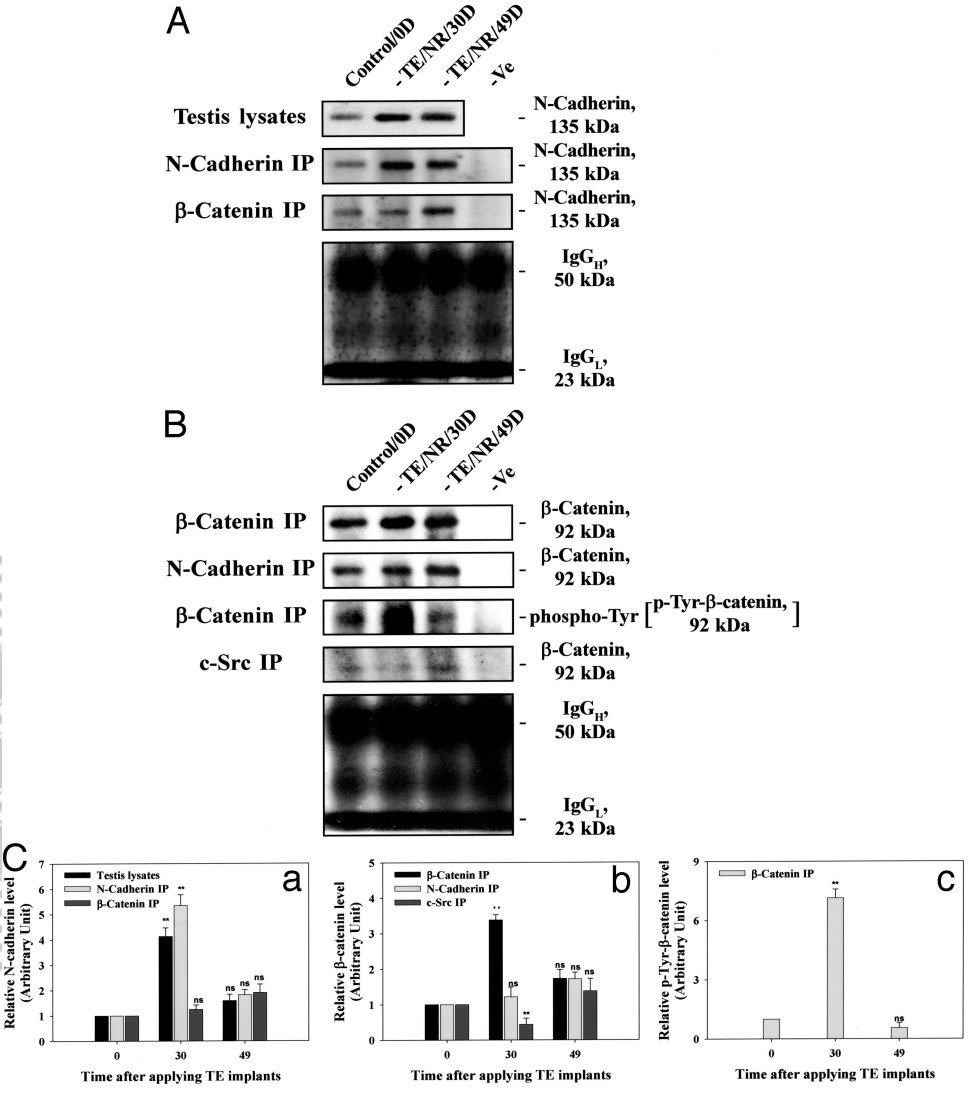

FIG. 9. A study using co-IP to assess changes in the association between N-cadherin and β-catenin, and β-catenin phosphorylation status during androgen suppression-induced germ cell loss and its recovery. Co-IP using lysates from normal rat testes and spontaneous natural recovery on d 30 and 49 was performed as described in *Materials and Methods*. Proteins were resolved by SDS-PAGE on 7.5% *T* SDS-polyacrylamide gels and transferred to nitrocellulose papers, and blots were incubated with N-cadherin, β-catenin, and phospho-Tyr antibody. For negative control, IgG of the corresponding species was used for co-IP. A, Testis lysates were used as positive controls. N-Cadherin was shown to lose its ability to interact with β-catenin at the time of germ cell loss (middle lane *vs.* the other two lanes), but this protein-protein association was reestablished in the recovery phase (right lane *vs.* the other two lanes). B, The observation in A was confirmed when the co-IP products from different experiments were immunoblotted using an anti-β-catenin antibody or a phospho-Tyr antibody. The *bottom* panels in A and B illustrate the heavy and the light chains of IgG, which served as loading controls. C, Histogram prepared using blots, such as those shown in A and B, with n = 3; a–c, levels of N-cadherin, β-catenin, and phospho-Tyr-β-catenin that were pulled down by antibodies against different target proteins to assess changes in protein-protein interactions during androgen suppression-induced germ cell loss and recovery. Data were normalized against control lysates, which were arbitrarily set at 1. ns, not significantly different from 0 h by Student's *t* test; **, significantly different at $P < 0.01$.

used this hormonal withdrawal model to reevaluate these earlier results with several unexpected findings.

First, it has been known for decades that T produced by Leydig cells under the regulation of LH is essential to spermatogenesis (for reviews, see Refs. 12, 48). TE implants that induce a supra-T level in the systemic circulation can suppress the intratesticular T level. This, in turn, causes detachment of step 8 spermatids and beyond from Sertoli cells in the seminiferous epithelium, so that spermatids are released prematurely to the tubule lumen (for reviews, see Refs. 12, 15). When the testicular T level is restored either by T implants that replace the TE implants or simply by TE implant removal to permit naturally spontaneous recovery, cell adhesion function and spermatogenesis can be restored. Thus, this model was used in this study. Interestingly, it was reported that actin bundles found between the Sertoli cell membrane and smooth endoplasmic reticulum at the site of apical ES remained qualitatively normal during TE treatment that depleted endogenous T level in the testis (47). This observation is significant because it suggests that cell adhesion molecules at the apical ES *per se* are the target of this treatment rather than the underlying cytoskeleton. It is also possible that changes in the cell adhesion function of these ES-structural proteins can contribute to the detachment of germ cells from the epithelium rather than an extensive restructuring of the ES structural protein/actin cytoskeleton complex. Indeed, it was shown in our studies that the event of germ cell loss during intratesticular T suppression induced by TE implants correlated to a loss of protein-protein interactions between cadherins and catenins as well as between c-Src and β-catenin. Perhaps most importantly, it is apparent that such a loss of protein-protein interaction is the result of an increase in Tyr phosphorylation of β-catenin. This is consistent with the findings based on studies in other epithelia that an increase in β-catenin phosphorylation can affect cell adhesion function of the cadherin/catenin protein complex (for reviews, see Refs. 2, 3, 49, 50). This is likely mediated by c-Src, which is a nonreceptor protein tyrosine kinase. It is plausible that once c-Src induces phosphorylation of β-catenin, it is dissociated from the cadherin/catenin protein complex, which also explains the surge in c-Src (to induce β-catenin phosphorylation) and its loss of association with β-catenin (when it finishes its job) at the time of germ cell loss. Second, it was observed that many phosphatases, kinases,

balt3/zee-end/zee-end/zee00305/zee0730-05a | hurtr | S=12 | 1/21/05 | 7:52 | 4/Color Figure(s): 1,2,3,6,10 | Art: 1195093 | Input-lc

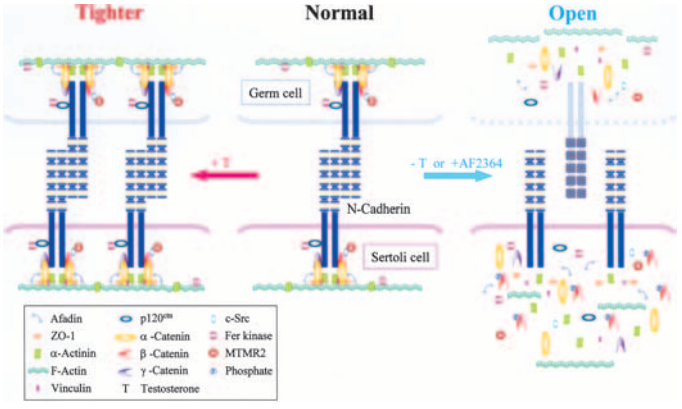

FIG. 10. A schematic drawing illustrating that a loss of protein-protein interaction in the cadherin/catenin/cSrc/MTMR2 protein complex as well as its interaction with other peripheral proteins can induce germ cell loss from the seminiferous epithelium. The loss of cell adhesion function between Sertoli cells and spermatids at the ES site can be caused by a decline in the endogenous T level in the testis after TE implants were placed under the skin in adult rats. It is of interest to note that an increase in the levels of N-cadherin and β-catenin were detected regardless of whether the endogenous T level in the testis was induced or reduced. Yet a decline in endogenous T level can lead to a loss of protein-protein interactions between N-cadherin and β-catenin as well as between β-catenin and c-Src as reported herein, even though the levels of these proteins were significantly induced in the epithelium. This is possibly the result of a reduced Tyr phosphorylation of β-catenin. This in turn leads to a loss of adaptor function (note that β-catenin is a putative adaptor) and failure to recruit signaling molecules and other adaptors to the AJ site and to anchor the cadherin/catenin complex to the actin cytoskeleton. This thus leads to a disruption of AJ (see *right vs. middle*). However, an increase in endogenous T level has no disruptive effects on interactions between N-cadherin and β-catenin and their association with the peripheral proteins; therefore, an increase in their protein levels helps to stabilize AJs further, making them tighter (see *left vs. middle*).

and adaptors, as well as integral membrane proteins that were examined in this androgen-suppression model, were induced at the time of germ cell loss, consistent with the trend found in the AF-2364 model (13, 32, 38, 43, 46). Collectively, these results suggest that the mechanisms that induce germ cell loss from the epithelium in both models are similar and that the signaling pathways that were shown to regulate AJ dynamics in the seminiferous epithelium are not nonspecific toxic effects of AF-2364. The fact that the effects of AF-2364 in inducing germ cell loss are much more rapid than the TE-induced affects, 1–7 d *vs.* 15–30 d, seemingly suggests that AF-2364 is a more potent chemical entity to induce germ cell loss *vs.* the androgen suppression-induced changes in the epithelium. Needless to say, much work remains to be done to delineate the downstream action of the signaling pathways that regulate Sertoli-germ cell attachment during spermatogenesis. From the findings reported herein, one of these mechanisms is mediated via changes in protein-protein interactions of the cell adhesion molecules at the Sertoli cell-spermatid interface.

MTMR2 structurally interacts with c-Src but not PI 3-K p85α in the rat testis

MTMR2 is a member of the MTM family of phosphatase/pseudophosphatase with a PTP/dual specific phosphatase catalytic site, CX_5R (for a review, see Ref. 18). It can dephosphorylate phosphatidylinositol 3-phosphate and phosphatidylinositol 3,5-bisphosphate at D3-phosphate (20). MTMR2 is also highly expressed in the testis (22), and its level in the testis is significantly induced during maturation or during Sertoli-germ cell AJ assembly using cells cocultured *in vitro* (22, 23). Furthermore, a case study in which a CMT 4B patient was azoospermic (18), along with MTMR2$^{-/-}$ mice being found to have defects in retaining spermatids in the epithelium, have illustrated its significance in spermatogenesis. Interestingly, MTMR2$^{-/-}$ mice at 4–6 months of age were azoospermic, in which more than 90% of the tubules were devoid of elongating/elongate and round spermatids in the seminiferous epithelium, leading to a significant reduction in testicular weight and size by approximately 30–40% *vs.* normal mice (24). Herein MTMR2 was shown to be induced significantly during AJ disruption after AF-2364 or TE implant treatment, and MTMR2 was localized to the apical ES in the epithelium, further supporting the notion that it may play a crucial role in ES dynamics during spermatogenesis. In the brain, or kidney 293 cells, at least three putative binding partners of MTMR2 have been identified thus far. First, MTMR5 (26), a catalytically inactive MTM protein, may function as an adaptor and/or enhancer that guides MTMR2 to the specific subcellular localization as well as enhances its phosphatase activity by acting as a binding partner (26). Other studies have shown that MTMR5$^{-/-}$ mice were azoospermic, similar to MTMR2$^{-/-}$ mice, where germ cells lost their ability to attach to the seminiferous epithelium (51), suggesting this MTMR2/MTMR5 protein complex may be an important regulator of AJ dynamics in the testis. Second, neurofilament light chain protein, a neurofilament protein that associates with CMT 2E, a neuropathological condition typified by axonal losses, is structurally associated with MTMR2, and they appear to be crucial for signal transmission along the nerve fibers (27). Third, Dlg1 (also known as synapse-associated protein-97) (24), a scaffolding molecule with a putative PDZ (PSD95/DLG/ZO-1) domain, is expressed in brain and testes, as well as in several junction types (52). Interestingly, in studies by co-IP to identify the putative binding partner(s) of MTMR2 in the testis, it was shown that lipid phosphatase MTMR2 interacted with nonreceptor protein tyrosine kinase c-Src instead of the adaptor subunit p85α of PI 3-K. This is somewhat unexpected because PI 3-K is a lipid and protein kinase and is apparently a natural interacting partner of MTMR2. Yet a recent report has shown that a substrate-trapped mutant of MTM1 (MTM1 belongs to the MTM family having the highest homology with MTMR2), but not the wild-type MTM1, can interact with VPS 34, a class III PI 3-K (53), supporting the notion that PI 3-K is not the likely natural interacting partner of MTMR2. Interestingly, proteins that are Tyr phosphorylated by exogenously expressed c-Src cannot be reversely dephosphorylated when coexpressing with MTM1, yet they can be dephosphorylated by other protein phosphatases, such as PTP-PEST (PTP rich in Pro, Glu, Ser and Thr) and TC-PTP (T-cell PTP), in yeasts (53). This seemingly suggests that MTMs, such as MTM1, may not use c-Src as a binding partner to form a regulatory unit similar to the MTMR2-c-Src complex identified in the rat testis. However, the interaction of

AQ: J

balt3/zee-end/zee-end/zee00305/zee0730-05a | hurtr | S=12 | 1/21/05 | 7:52 | 4/Color Figure(s): 1,2,3,6,10 | Art: 1195093 | Input-lc

MTM and other kinases may be regulated either via a lipid second messenger, such as phosphatidylinositol 5-phosphate, a product of MTMR2 that may increase the enzymatic activity of MTMs (20) or a yet-to-be identified adaptor. Another surprising finding is that because MTMR2 has a PDZ-binding domain near its C-terminus, and it can interact with the PDZ domain of Dlg1 in COS-7 cells (24), it is expected to interact with other proteins having the PDZ domain at the ES. Yet MTMR2 failed to interact with zonula occludens 1 (ZO-1), another PDZ-domain-containing protein, as reported herein. Additionally, MTMR2 failed to interact with α-actinin, another lipid-associated adaptor and an actin-binding and bundling protein. These findings also illustrate that among many adaptors and kinases that were identified in the apical ES, only c-Src physically interacts with MTMR2 in the seminiferous epithelium. This result obtained by co-IP was also confirmed by a colocalization study using fluorescent microscopy. Although MTMR2 failed to interact directly with the known adaptors at the apical ES, including ZO-1, α-actinin, p130Cas, Wiskott-Aldrich syndrome protein (WASP), and others, but interacted only with c-Src, it must be noted that c-Src was recently shown to associate with some of these adaptors such as Wiskott-Aldrich syndrome protein and the cadherin-catenin protein complex (13). As such, MTMR2 can still indirectly interact with other adaptors to affect cell adhesion function of the cadherin-catenin complex via c-Src, and this possibility must be vigorously investigated in future studies.

The MTMR2/c-Src complex regulates ES dynamics likely via its interaction with the cadherin/catenin protein complex

The cadherin/catenin, the integrin/laminin, and the nectin/afadin/ponsin protein complexes are the three currently known structural protein complexes that confer cell adhesion function in the seminiferous epithelium at the apical ES site (for reviews, see Refs. 2, 10). Other studies have shown that the phosphorylation status of these protein complexes, in particular the cadherin/catenin complex, is a determining factor to confer cell adhesion function (49). For instance, an increase in Tyr phosphorylation of the cadherin/catenin complex is associated with a loss of interaction between cadherin, catenin, and the actin cytoskeleton, leading to a loss of cell adhesion function (49, 50, 54). In earlier studies, an induction of N-cadherin and β-catenin was detected in the AF-2364 model (32, 43, 44) at the time of germ cell loss, similar to the results reported herein during TE treatment-induced germ cell loss. Yet it is not known from these earlier studies whether any changes in the phosphorylation status of these proteins indeed occurred. Furthermore, the cadherin/catenin complex was localized to both the basal and apical ES sites (32, 43, 55, 56) and was recently shown to interact with the c-Src/Csk/CK II kinase complex (13). Because both MTMR2 and c-Src were induced during TE treatment at the time of germ cell loss and both MTMR2 and the phosphorylated form of Src (p-Src-Tyr^{416}) were colocalized to the apical ES and to a lesser extent to the basal ES at stage VIII, together with the fact that c-Src is a binding partner of the cadherin/catenin protein complex, it seems logical to speculate that the cadherin/catenin protein complex may be the target of the MTMR2/c-Src complex. We have now shown that the N-cadherin/β-catenin protein complex was disassociated *in vivo* during androgen depletion-induced AJ disruption, accompanied by an increase in Tyr phosphorylation of β-catenin. This result is consistent with earlier reports in other *in vitro* systems (*e.g.* Madin Darby canine kidney cells) that a loss of cell adhesion function of the cadherin-based complex is mediated by an increase in β-catenin phosphorylation (49, 54). Interestingly, a decrease in c-Src association with β-catenin was also detected, suggesting that c-Src was moving away from β-catenin once it phosphorylated its substrate. It is obvious that the α6β1-integrin/laminin-γ3 complex can also be another target of the MTMR2/c-Src complex. For instance, it was recently shown that phospho-focal adhesion kinase-Tyr^{397} could bind to β1-integrin, vinculin, and c-Src (38, 46), suggesting c-Src may be the linker that associates MTMR2 with β1-integrin indirectly via phospho-focal adhesion kinase. There are also reports illustrating that Src and another lipid/protein phosphatase, PTEN (phosphatase and tensin homolog deleted on chromosome ten), can regulate integrin signaling (57, 58), supporting the notion that MTMR2/c-Src may regulate the integrin/laminin complex at the apical ES. In short, results of this study have clearly demonstrated that c-Src is a putative binding partner of MTMR2 in the testis, in particular at the apical ES, and the cadherin/catenin protein complex is one of its targets.

MTMR2 and c-Src can be induced by T in Sertoli-germ cell cocultures in vitro

Results of the *in vivo* study presented herein suggest that androgen plays a crucial role in regulating both MTMR2 and c-Src in the testis. To further confirm this observation, the levels of these proteins were quantified in Sertoli-germ cells cocultured *in vitro*. It was noted that both MTMR2 and c-Src were indeed induced by T in the cocultures, and this dose-dependent induction could be blocked by CPA, an antiandrogen (for a review, see Ref. 59). These data thus demonstrate unequivocally that both MTMR2 and c-Src, as well as cadherin as shown in an earlier study (32), were androgen-regulated proteins. However, much research is needed to understand how androgens regulate the interaction between these proteins, adaptors, and the cadherin/catenin complex.

Issues on changes in levels of target proteins (e.g. kinases, phosphatases, and adaptors) in the seminiferous epithelium as a result of germ cell loss

An interesting issue arises regarding results obtained from this androgen suppression model and the AF-2364 model that correlates changes in target proteins, such as MTMR2 and c-Src, with the event of germ cell loss from the seminiferous epithelium pertinent to AJ disruption. For instance, during the progressive loss of germ cells from the epithelium, the distribution of different cell types in the testis is altered at different time points in both models. This may confound our interpretation, at least to some extent, regarding changes in specific target proteins and/or genes by quantifying their

balt3/zee-end/zee-end/zee00305/zee0730-05a | hurtr | S=12 | 1/21/05 | 7:52 | 4/Color Figure(s): 1,2,3,6,10 | Art: 1195093 | Input-lc

steady-state protein and/or mRNA levels (for a review, see Ref. 60). For instance, if a protein, such as rMTMR2, is also produced by germ cells in the seminiferous epithelium (22), an induction of this protein during germ cell loss as quantified by immunoblotting was likely an underestimate because the cytosol that was being analyzed had been contributed largely by Sertoli cells and other somatic cells (*e.g.* peritubular myoid and Leydig cells) instead of germ cells as in normal testes, even though the same amount of protein was being analyzed (and the blot was reprobed with an anti-actin antibody staining to assess equal protein loading). However, this is an inherent problem with these models, which is somewhat difficult to resolve. First, although we had done some preliminary kinetic studies to assess the loss of different germ cell types (*e.g.* elongate, elongating, and round spermatids and spermatocytes), after AF-2364 treatment, which showed that elongate/elongating spermatids were depleted from the epithelium much more rapidly than round spermatids and spermatocytes (6.5 h *vs.* 3–6 d) (44), we do not have detailed morphometric analysis results on the time-dependent loss of specific germ cell types in both models to correlate these changes to each treatment regimen in either model. Even if these studies were completed, each animal would still respond differently, and there would have been variations between animals responding to the same treatment. Second, although germ cells were depleted from the epithelium, they probably would still be included in the immunoblot analysis because many germ cells would still be in the tubule lumen, in particular in the early phase of germ cell loss. As such, it is important to use other approaches to confirm changes of a specific target protein (*e.g.* MTMR2) in the epithelium during germ cell loss, such as with the use of immunohistochemistry and fluorescent microscopy as reported herein.

Another concern related to the data interpretation using these models is that an induction of a target protein, either a kinase, a phosphatase, or an adaptor, is in fact the result of AJ disruption rather than a reflection of germ cell loss. The best argument against this possibility is the result of studies using inhibitors. For instance, it was shown that Sertoli-germ cell AJ dynamics are regulated by the β1-integrin/RhoB/ Rho-associated protein kinase/LIMK (*L*in-11 *I*sl-1 *M*ec3 *k*inase/cofilin signaling pathway (61) and the β1-integrin/ laminin-γ3/membrane-type 1 matrix metalloproteinase/ matrix metalloproteinase 2 protein complex (46) because these proteins were significantly induced during AF-2364-mediated germ cell loss from the epithelium. Indeed, the use of either Y27632, a specific inhibitor for Rho-associated protein kinase or 2R-2-[(4-biphenylylsulfonyl)amino]-3-phenylpropionic acid, an inhibitor against matrix metalloproteinase 2, could significantly delay the AF-2364-induced germ cell loss from the epithelium (46, 61), validating these interpretations. Likewise, an induction of the MTMR2/c-Src protein complex as reported herein can indeed induce an increase in β-catenin phosphorylation, which plausibly leads to a loss of protein-protein interactions between N-cadherin and β-catenin protein as confirmed by experiments using co-IP, thereby inducing germ cell loss from the epithelium.

AQ: Q

AQ: R

Summary and concluding remarks

In summary, we have demonstrated that MTMR2 is a stage-specific lipid phosphatase that is structurally associated with c-Src and that both proteins are colocalized to the apical ES at stage VIII of the epithelial cycle before spermiation. It is likely that the MTMR2/c-Src is an important protein complex that regulates the cell adhesion function of the cadherin/catenin complex via a lipid second messenger and possibly other adaptor(s) and/or kinases(s) by altering protein-protein interactions of the structural protein complexes at the ES site, facilitating cell movement during spermatogenesis.

Received September 7, 2004. Accepted December 1, 2004.

Address all correspondence and requests for reprints to: C. Yan Cheng, Ph.D., Population Council, 1230 York Avenue, New York, New York 10021. E-mail: Y-cheng@popcbr.rockefeller.edu.

This work was supported in part by grants from the National Institutes of Health (National Institute of Child Health and Human Development, U01 HD045908 and U54 HD029990, Project 3, to C.Y.C.), the Contraceptive Research and Development (CONRAD) Program (Consortium for Industrial Collaboration in Contraceptive Research, CICCR CIG 01-72 and CIG 96-05-B to C.Y.C. and CIG-01-74 to D.D.M.), and Hong Kong Research Grant Council (HKU 7194/01M and 7413/04M to W.M.L. and C.Y.C.).

AQ: S

References

1. **de Kretser DM, Loveland KL, Meinhardt A, Simorangkir D, Wreford N** 1998 Spermatogenesis. Hum Reprod 13:1–8
2. **Cheng CY, Mruk DD** 2002 Cell junction dynamics in the testis: Sertoli-germ cell interactions and male contraceptive development. Physiol Rev 82:825–874
3. **Mruk DD, Cheng CY** 2004 Sertoli-Sertoli and Sertoli-germ cell interactions and their significance in germ cell movement in the seminiferous epithelium during spermatogenesis. Endocr Rev 25:747–806
4. **Mruk D, Cheng C** 2004 Cell-cell interactions at the ectoplasmic specialization in the testis. Trends Endocrinol Metabol 15:439–447
5. **Silvestrini B, Palazzo G, De Gregorio M** 1984 Lonidamine and related compounds. Prog Med Chem 21:111–135
6. **Cheng CY, Silvestrini B, Grima J, Mo MY, Zhu LJ, Johansson E, Saso L, Leone MG, Palmery M, Mruk DD** 2001 Two new male contraceptives exert their effects by depleting germ cells prematurely from the testis. Biol Reprod 65: 449–461
7. **Grima J, Silvestrini B, Cheng CY** 2001 Reversible inhibition of spermatogenesis in rats using a new male contraceptive, 1-(2,4-dichlorobenzyl)-indazole-3-carbohydrazide. Biol Reprod 64:1500–1508
8. **Cheng CY, Mruk DD, Silvestrini B, Bonanomi M, Wong CH, Siu MKY, Lee NPY, Mo MY,** AF-2364 [1-(2,4-dichlorobenzyl)-indazole-3-carbohydrazide] is a potential male contraceptive in adult rats: a review of recent data. Contraception, in press
9. **Siu MK, Cheng CY** 2004 Dynamic cross-talk between cells and the extracellular matrix in the testis. Bioessays 26:978–992
10. **Lee NPY, Cheng CY** 2004 Ectoplasmic specialization, a testis-specific cell-cell actin-based adherens junction type: is this a potential target for male contraceptive development? Human Reprod Update 10:349–369
11. **Lui WY, Mruk DD, Lee WM, Cheng CY** 2003 Adherens junction dynamics in the testis and spermatogenesis. J Androl 24:1–14
12. **McLachlan RI, O'Donnell L, Meachem SJ, Stanton PG, de K, Pratis K, Robertson DM** 2002 Hormonal regulation of spermatogenesis in primates and man: insights for development of the male hormonal contraceptive. J Androl 23:149–162
13. **Lee NPY, Cheng CY** 2005 Protein kinases and adherens junction dynamics in the seminiferous epithelium of the rat testis. J Cell Physiol 202:344–360
14. **Turner TT, Jones CE, Howards SS, Ewing LL, Zegeye B, Gunsalus GL** 1984 On the androgen microenvironment of maturing spermatozoa. Endocrinology 115:1925–1932
15. **McLachlan RI, Wreford N, O'Donnell L, de Kretser DM, Robertson DM** 1996 The endocrine regulation of spermatogenesis: independent roles for testosterone and FSH. J Endocrinol 148:1–9
16. **Bolino A, Muglia M, Conforti FL, LeGuern E, Salih MA, Georgiou DM, Christodoulou K, Hausmanowa-Petrusewicz I, Mandich P, Schenone A, Gambardella A, Bono F, Quattrone A, Devoto M, Monaco AP** 2000 Charcot-Marie-Tooth type 4B is caused by mutations in the gene encoding myotubularin-related protein-2. Nat Genet 25:17–19
17. **Begley MJ, Taylor GS, Kim SA, Veine DM, Dixon JE, Stuckey JA** 2003 Crystal

AQ: T

balt3/zee-end/zee-end/zee00305/zee0730-05a | hurtr | S=12 | 1/21/05 | 7:52 | 4/Color Figure(s): 1,2,3,6,10 | Art: 1195093 | Input-lc

structure of a phosphoinositide phosphatase, MTMR2: insights into myotubular myopathy and Charcot-Marie-Tooth syndrome. Mol Cell 12:1391–1402
18. **Laporte J, Bedez F, Bolino A, Mandel JL** 2003 Myotubularins, a large disease-associated family of cooperating catalytically active and inactive phosphoinositides phosphatases. Hum Mol Genet 12:R285–R292
19. **Berger P, Bonneick S, Willi S, Wymann M, Suter U** 2002 Loss of phosphatase activity in myotubularin-related protein 2 is associated with Charcot-Marie-Tooth disease type 4B1. Hum Mol Genet 11:1569–1579
20. **Schaletzky J, Dove SK, Short B, Lorenzo O, Clague MJ, Barr FA** 2003 Phosphatidylinositol-5-phosphate activation and conserved substrate specificity of the myotubularin phosphatidylinositol 3-phosphatases. Curr Biol 13:504–509
21. **Nandurkar HH, Huysmans R** 2002 The myotubularin family: novel phosphoinositide regulators. IUBMB Life 53:37–43
22. **Li JC, Samy ET, Grima J, Chung SS, Mruk DD, Lee WM, Silvestrini B, Cheng CY** 2000 Rat testicular myotubularin, a protein tyrosine phosphatase expressed by Sertoli and germ cells, is a potential marker for studying cell-cell interactions in the rat testis. J Cell Physiol 185:366–385
23. **Li JC, Lee WM, Mruk DD, Cheng CY** 2001 Regulation of Sertoli cell myotubularin (rMTM) expression by germ cells *in vitro*. J Androl 22:266–277
24. **Bolino A, Bolis A, Previtali SC, Dina G, Bussini S, Dati G, Amadio S, Carro UD, Mruk DD, Feltri ML, Cheng CY, Quattrini A, Wrabetz L** 2004 Disruption of *Mtmr2* produces CMT4B1-like neuropathy with myelin outfolding and impaired spermatogenesis. J Cell Biol 167:711–721
25. **Berger P, Schaffitzel C, Berger I, Ban N, Suter U** 2003 Membrane association of myotubularin-related protein 2 is mediated by a pleckstrin homology-GRAM domain and a coiled-coil dimerization module. Proc Natl Acad Sci USA 100:12177–12182
26. **Kim SA, Vacratsis PO, Firestein R, Cleary ML, Dixon JE** 2003 Regulation of myotubularin-related (MTMR)2 phosphatidylinositol phosphatase by MTMR5, a catalytically inactive phosphatase. Proc Natl Acad Sci USA 100:4492–4497
27. **Previtali SC, Zerega B, Sherman DL, Brophy PJ, Dina G, King RH, Salih MM, Feltri L, Quattrini A, Ravazzolo R, Wrabetz L, Monaco AP, Bolino A** 2003 Myotubularin-related 2 protein phosphatase and neurofilament light chain protein, both mutated in CMT neuropathies, interact in peripheral nerve. Hum Mol Genet 12:1713–1723
28. **Zwain IH, Cheng CY** 1994 Rat seminiferous tubular culture medium contains a biological factor that inhibits Leydig cell steroidogenesis: its purification and mechanism of action. Mol Cell Endocrinol 104:213–227
29. **Cheng CY, Mather JP, Byer AL, Bardin CW** 1986 Identification of hormonally responsive proteins in primary Sertoli cell culture medium by anion-exchange high performance liquid chromatography. Endocrinology 118:480–488
30. **Grima J, Pineau C, Bardin CW, Cheng CY** 1992 Rat Sertoli cell clusterin, α_2-macroglobulin, and testins: biosynthesis and differential regulation by germ cells. Mol Cell Endocrinol 89:127–140
31. **Galdieri M, Ziparo E, Palombi F, Russo MA, Stefanini M** 1981 Pure Sertoli cell cultures: a new model for the study of somatic-germ cell interactions. J Androl 2:249–254
32. **Lee NPY, Mruk DD, Lee WM, Cheng CY** 2003 Is the cadherin/catenin complex a functional unit of cell-cell actin-based adherens junctions in the rat testis? Biol Reprod 68:489–508
33. **Lee NPY, Cheng CY** 2003 Regulation of Sertoli cell tight junction in the rat testis via the nitric oxide synthase/soluble guanylate cyclase/cyclic guanosine monophosphate/protein kinase G signaling pathway: an *in vitro* study. Endocrinology 144:3114–3129
34. **Aravindan GR, Pineau CP, Bardin CW, Cheng CY** 1996 Ability of trypsin in mimicking germ cell factors that affect Sertoli cell secretory function. J Cell Physiol 168:123–133
35. **Wong CCS, Chung SSW, Grima J, Zhu LJ, Mruk DD, Lee WM, Cheng CY** 2000 Changes in the expression of junctional and nonjunctional complex component genes when inter-Sertoli tight junctions are formed *in vitro*. J Androl 21:227–237
36. **Lui WY, Mruk DD, Cheng CY** 2005 Interactions among IQGAP1, Cdc42, and the cadherin/catenin protein complex regulate Sertoli-germ cell adherens junction dynamics in the testis. J Cell Physiol 202:49–66
37. **Cameron DF, Muffly KE** 1991 Hormonal regulation of spermatid binding. J Cell Sci 100:623–633
38. **Siu MKY, Mruk DD, Lee WM, Cheng CY** 2003 Adhering junction dynamics in the testis are regulated by an interplay of β1-integrin and focal adhesion complex-associated proteins. Endocrinology 144:2141–2163
39. **Grima J, Zhu LJ, Zong SD, Catterall JF, Bardin CW, Cheng CY** 1995 Rat testin is a newly identified component of the junctional complexes in various tissues whose mRNA is predominantly expressed in the testis and ovary. Biol Reprod 52:340–355
40. **Bradford MM** 1976 A rapid and sensitive method for the quantitation of microgram quantities of protein utilizing the principle of protein-dye binding. Anal Biochem 72:248–254
41. **Laemmli UK** 1970 Cleavage of structural proteins during the assembly of the head of bacteriophage T4. Nature 227:680–685
42. **Lui WY, Wong CH, Mruk DD, Cheng CY** 2003 TGF-β3 regulates the blood-testis barrier dynamics via the p38 mitogen activated protein (MAP) kinase pathway: an *in vivo* study. Endocrinology 144:1139–1142
43. **Lee NPY, Mruk DD, Conway AM, Cheng CY** 2004 Zyxin, axin, and Wiskott-Aldrich syndrome protein are adaptors that link the cadherin/catenin protein complex to the cytoskeleton at adherens junctions in the seminiferous epithelium of the rat testis. J Androl 25:200–215
44. **Chen YM, Lee NPY, Mruk DD, Lee WM, Cheng CY** 2003 Fer kinase/FerT and adherens junction dynamics in the testis: an *in vitro* and *in vivo* study. Biol Reprod 69:656–672
45. **O'Donnell L, McLachlan RI, Wreford NG, Robertson DM** 1994 Testosterone promotes the conversion of round spermatids between stages VII and VIII of the rat spermatogenic cycle. Endocrinology 135:2608–2614
46. **Siu MKY, Cheng CY** 2004 Interactions of proteases, protease inhibitors, and the β1 integrin/laminin γ3 protein complex in the regulation of ectoplasmic specialization dynamics in the rat testis. Biol Reprod 70:945–964
47. **O'Donnell L, Stanton PG, Bartles JR, Robertson DM** 2000 Sertoli cell ectoplasmic specializations in the seminiferous epithelium of the testosterone-suppressed adult rat. Biol Reprod 63:99–108
48. **Kamischke A, Nieschlag E** 2004 Progress towards hormonal male contraception. Trends Pharmacol Sci 25:49–57
49. **Gumbiner BM** 2000 Regulation of cadherin adhesive activity. J Cell Biol 148:399–404
50. **Daniel JM, Reynolds AB** 1997 Tyrosine phosphorylation and cadherin/catenin function. Bioessays 19:883–891
51. **Firestein R, Nagy PL, Daly M, Huie P, Conti M, Cleary ML** 2002 Male infertility, impaired spermatogenesis, and azoospermia in mice deficient for the pseudophosphatase Sbf1. J Clin Invest 109:1165–1172
52. **Muller BM, Kistner U, Veh RW, Cases-Langhoff C, Becker B, Gundelfinger ED, Garner CC** 1995 Molecular characterization and spatial distribution of SAP97, a novel presynaptic protein homologous to SAP90 and the *Drosophila* discs-large tumor suppressor protein. J Neurosci 15:2354–2366
53. **Blondeau F, Laporte J, Bodin S, Superti-Furga G, Payrastre B, Mandel JL** 2000 Myotubularin, a phosphatase deficient in myotubular myopathy, acts on phosphatidylinositol 3-kinase and phosphatidylinositol 3-phosphate pathway. Hum Mol Genet 9:2223–2229
54. **Gooding JM, Yap KL, Ikura M** 2004 The cadherin-catenin complex as a focal point of cell adhesion and signalling: new insights from three-dimensional structures. Bioessays 26:497–511
55. **Wine RN, Chapin RE** 1999 Adhesion and signaling proteins spatiotemporally associated with spermiation in the rat. J Androl 20:198–213
56. **Johnson KJ, Boekelheide K** 2002 Dynamic testicular adhesion junctions are immunologically unique. II. Localization of classic cadherins in rat testis. Biol Reprod 66:992–1000
57. **Tamura M, Gu J, Tran H, Yamada KM** 1999 PTEN gene and integrin signaling in cancer. J Natl Cancer Inst 91:1820–1828
58. **Felsenfeld DP, Schwartzberg PL, Venegas A, Tse R, Sheetz MP** 1999 Selective regulation of integrin-cytoskeleton interactions by the tyrosine kinase Src. Nature Cell Biol 1:200–206
59. **Berrevoets CA, Umar A, Brinkmann AO** 2002 Antiandrogens: selective androgen receptor modulators. Mol Cell Endocrinol 198:97–103
60. **Ivell R, Spiess A** 2002 Analysing differential gene expression in the testis. Berlin: Springer-Verlag
61. **Lui WY, Lee WM, Cheng CY** 2003 Sertoli-germ cell adherens junction dynamics in the testis are regulated by RhoB GTPase via the ROCK/LIMK signaling pathway. Biol Reprod 68:2189–2206

Endocrinology **is published monthly by The Endocrine Society (http://www.endo-society.org), the foremost professional society serving the endocrine community.**